nature portfolio

Peer Review File

Light-matter coupling via quantum pathways for spontaneous symmetry breaking in vdW antiferromagnetic semiconductors

Corresponding Author: Dr Byung Cheol Park

This file contains all reviewer reports in order by version, followed by all author rebuttals in order by version.

Version 0:

Reviewer comments:

Reviewer #1

(Remarks to the Author)
The manuscript reports the emergence of birefringence and linear dichroism in FePS3 below Neel temperature, and the authors ascribe these emergent anisotropies to the different quantum interferences between the light induced quantum pathways through Fe d-d orbital transitions and spin sector in two directions. At the end, a Maxican hat potential is shown to explain the phase transition. I find the results and interpretation very interesting, but have some questions on this stage before I can recommend publication in Nature communications.

Man concerns:
(1) The authors didn't perform a pump-probe experiment, where the pump induces birefringence/linear dichroism effects and the probe detects them. Here, the authors only reveal these effects using light, right? In my opinion, the emergence of the birefringence and linear dichroism below Neel temperature is due to the anisotropic AFM order, and these anisotropic effects should be the intrinsic properties of the materials, which don't rely on the light-matter interaction. Even if there is no light shining on the sample, these effects should exist as well. Involving quantum interference to explain the data is interesting, but may not be necessary.
(2) In Fig5 the phases for different samples remain the same, but I don't understand why the amplitude of the effects depends on the thickness as they should be the intrinsic properties of the materials. Is it possible that the sample thickness was not taken into consideration during the calculation of n and k.
(3) The manuscript writes "We note that the Raman data do not show any change, ruling out the possibility of structural phase transition-induced anisotropy." However, this AFM transition is related the structural distortion as demonstrated in Nature 620, 988-993 (2023) and Nature communication 13, 6598 (2022).

Small suggestions
(4) I have some small suggestions on the introduction part. The author may want to generalize this quantum interference from linear optics to non-linear optics, such as second harmonic generation (SHG). There may be a few contributions (magnetic and electric dipole) to SHG and these contributions can have interference and give rise a quantum phase, for example in Nature materials 23, 790–795 (2024), where an electronic polarization is induced by light.
(5) The manuscript presents 6 figures in total and only 3 of them are experimental data. The authors may put 1-2 into Supplementary material to shorten the length.

Reviewer #2

(Remarks to the Author)
This study investigates light-matter interaction induced quantum anisotropy in van der Waals (vdW) antiferromagnetic (AFM) semiconductors, particularly FePS3, focusing on the quantum interference between light-induced quantum pathways. The interaction causes spontaneous symmetry breaking of dipole moments and leads to phenomena such as birefringence and linear dichroism below the Néel temperature. While the manuscript offers valuable insights, several revisions and clarifications are necessary before publication.

1. The emerging of birefringence and linear dichroism in FePS3 is already known due to spin-charge coupling in AFM semiconductors (Nano Lett. 21, 6938–6945 (2021), Nature Photonics 16, no. 4, 311-317 (2022)). The authors need to better articulate the significance of observing quantum interference and, consequently, LB and LD in FePS3 crystal.
2. The authors mention "quantum interference, which is further enhanced by the thickness effect," on page 2, line 12. Figure 5 shows the difference in linear birefringence (LB) and linear dichroism (LD) depending on the thickness. However, the authors should explain what types of enhancement can be observed. Is it just an increased value of LB and LD? If the crystal's thickness increases to bulk or decreases to a monolayer, is it possible to observe more increased or decreased values of LB and LD? Furthermore, it is unconventional to observe a significant difference in refractive index depending on the thickness of the material. The authors proposed "a synergy between quantum interference and thickness". However, the authors should provide more evidence of the enhancement caused by longer optical path-induced quantum interference
3. The refractive index and extinction coefficient are functions of wavelength, and it is conventional to report the LB and LD values as a function of wavelength. (Nat. Photonics 12, 392–396 (2018), Nature Communications volum, 12, Article number: 854 (2021)). According to the definition of quantum anisotropy in this paper, all other birefringent crystals should exhibit quantum anisotropy. The authors should clarify the definitions of conventional and quantum anisotropy.
4. Is it fair to assume that path1 and path2 have the same resonance frequency with only the phase difference of two electric dipoles, and simplify the model on page 4, lines 23-24? What is the evidence that both path 1 and path 2 have the same resonance frequency?
5. The authors need to articulate the adequacy of using only one Lorentz oscillator model to describe this system's quantum interference. As shown in Figures 3a and 5a, multiple oscillations can be observed in the experimental data, particularly at low temperatures. In this regard, the authors should consider the possibility that a simplified model is the reason for the observed deviation from the Lorentzian shape in the Δn and Δk lineshapes below the Néel temperature, as mentioned on page 6, lines 14-15. What if the authors use multiple Lorentz oscillators for modeling? Can they observe multiple Lorentzian shapes below the Néel temperature?
6. The authors should provide more detail about obtaining of n, k value. The authors used six oscillators to describe the dielectric function of the material, which is contradictory to using only one Lorentz oscillator for modeling the quantum interference.
7. The authors need to clarify the origin of the red/blue shift of the Lorentzian peak depending on the thickness in Figures 5c and d. Furthermore, the fitted Lorentzian peak does not match the experimental data, especially in Figure 5c.
8. For minor points, the referencing style should be consistent throughout the manuscript.

Version 1:

Reviewer comments:

Reviewer #1

(Remarks to the Author)
I appreciate the authors' detailed responses and their efforts in revising the manuscript based on my feedback. In both the response and the revised manuscript, the authors have effectively elaborated on the thickness and wavelength dependence of the refractive index, as well as the role of quantum interference effects in this material during light-matter interactions. The revised manuscript is also well-organized and more comprehensible than the previous version. I believe that all my concerns have been thoroughly addressed, and I am confident that this work will make a significant contribution to the field of light-matter interaction, both in the linear and non-linear regimes. Therefore, I recommend the manuscript for publication in Nature Communications.

Reviewer #2

(Remarks to the Author)
The authors have adequately addressed most of my comments. However, to fully address comment #2, the authors need to demonstrate the quantum interference effect experimentally in both a very thin sample (nearly monolayer) and a thick sample (approximately 1 μm). Currently, Fig 4 and S11 include only three data points (128 nm, 156 nm, and 431 nm), which is insufficient for a reliable linear fit in Fig S11. I recommend adding more data points, particularly at the extreme thicknesses, to strengthen the analysis. After this modification, I can recommend the work for publication.

Version 2:

Reviewer comments:

Reviewer #2

(Remarks to the Author)
I appreciate the authors' thorough responses and their efforts in revising the manuscript based on my feedback. They successfully demonstrated quantum interference across a wide range of $FePS_3$ thicknesses and further strengthened their arguments. Therefore, I recommend the manuscript for publication in Nature Communications.

Reviewer #1 (Remarks to the Author):

The manuscript reports the emergence of birefringence and linear dichroism in FePS3 below Neel temperature, and the authors ascribe these emergent anisotropies to the different quantum interferences between the light induced quantum pathways through Fe d-d orbital transitions and spin sector in two directions. At the end, a Maxican hat potential is shown to explain the phase transition. I find the results and interpretation very interesting, but have some questions on this stage before I can recommend publication in Nature communications.

Reply) Through all the comments, we felt the professionalism of the reviewer. To show our respect, we prepared to revise the manuscript based on the valuable comments. As a result of your feedback, our manuscript has been refined and now may be appropriate for publication in Nature Communications. We are convinced that this type of author-reviewer collaboration results in significant scientific advancement.

We appreciate your concern regarding the intrinsic nature of n and k. As you correctly pointed out, the anisotropic n and k observed in $FePS_3$ below TN arise from classical anisotropy due to AFM spin ordering. However, the quantum anisotropy we report is distinct from this classical effect. Quantum anisotropy leads to a thickness-dependent behavior of n and k, unlike the intrinsic nature of n and k in the absence of quantum interference.

To clarify this distinction, we have provided the following evidence:

1. **Intrinsic Behavior Above TN:** We demonstrate that n and k are thickness-independent above TN for all three samples.
2. **Quantum Interference Regime:** We identify a spectral region where quantum interference leads to thickness-dependent n and k.
3. **Classical Regime:** We show that outside the quantum interference region (below 1.4 eV and above 2.4 eV), n and k remain thickness-independent, exhibiting classical behavior.

For a detailed discussion, please refer to our responses to comments (1) and (2).

It was also a great chance to compare our steady-state measurement with transient pump-probe measurement data, which are compatible without any contradiction (see our reply to (3)). We also carefully revised the manuscript according to comments (4) for generalization to non-linear optics and (5) regarding reconstruction of the order) to improve the readability.

The authors sincerely thank you for your valuable feedback. Please see the detailed point-by-point response below.

Main concerns:

(1) The authors didn't perform a pump-probe experiment, where the pump induces birefringence/linear dichroism effects and the probe detects them. Here, the authors only reveal these effects using light, right? In my opinion, the emergence of the birefringence and linear dichroism below Neel temperature is due to the anisotropic AFM order, and these anisotropic effects should be the intrinsic properties of the materials, which don't rely on the light-matter interaction. Even if there is no light shining on the sample, these effects should exist as well. Involving quantum interference to explain the data is interesting, but may not be necessary.

(2) In Fig5 the phases for different samples remain the same, but I don't understand why the amplitude of the effects depends on the thickness as they should be the intrinsic properties of the materials. Is it possible that the sample thickness was not taken into consideration during the calculation of n and k.

Reply) We believe this comment is crucial and acknowledge that there may have been a misunderstanding. We apologize for the confusion. We will address comments (1) and (2) simultaneously in the following response.

To clarify our findings, we will distinguish between quantum anisotropy, which is an extrinsic property, and classical anisotropy, which is an intrinsic property. While quantum anisotropy is extrinsic in nature, it plays a crucial role in determining quantum phases of matter. Furthermore, its extrinsic nature offers opportunities to engineer and control quantum anisotropy, potentially leading to new quantum phases of matter.

To clarify this distinction, we have provided the following direct evidence:

1. Intrinsic Behavior Above TN (Fig. R1-1): We demonstrate that n and k are thickness-independent above TN for all three samples.

First, we would like to clarify that we have accurately measured and considered the thickness of each sample in our calculations of n and k.

2. Quantum Interference Regime Below TN (Fig. R1-2): We identify a spectral region where quantum interference leads to thickness-dependent n and k.

3. Classical Regime Below TN (Fig. R1-2): We show that outside the quantum interference region (above 2.4 eV, below 1.4 eV, unfortunately, the data quality is compromised due to limitations in our spectrometer's bandwidth.), n and k remain thickness-independent, exhibiting classical behavior.

Additionally, we have investigated the thickness dependence of n and k, which is a key finding that directly reflects the quantum interference effect. To directly address this issue, we present the full range of n and k spectra, which exhibit two distinct regions: with and without quantum interference (Fig. R1-2). **In the absence of quantum interference, as you correctly pointed out, the n and k spectra are identical for all sample thicknesses.** However, in the quantum interference region, the n and k spectra vary significantly across different thicknesses. [Importantly, the

quantum interference phase Φ_{QI} remains independent of thickness, showing its "real intrinsic" nature.] While the importance of intrinsic properties is widely recognized, the role of Φ_{QI} has been often overlooked in various fields of physics. This work underscores the significance of Φ_{QI} in fundamental physics.

We note that quantum anisotropy seems to be both intrinsic and extrinsic.

1) Intrinsic nature: When a photon is incident, two channels (dipole resonators) with their spectral overlap are simultaneously excited and therefore their quantum interference is inevitable, which seems to be intrinsic.
2) Extrinsic nature: As we have shown that quantum LB and LD are proportional to the sample thickness, quantum LB and LD are thickness-dependent like extrinsic properties. Nevertheless, quantum LB and LD are also distinct from purely extrinsic effects like multiple internal reflections that can be avoided by changing the thickness of the sample.

Such exotic nature of quantum LB and LD arises from the intrinsic character of the quantum interference effect. Their magnitude depends on the number of dipole moments (which is proportional to the thickness) involved in the quantum interference process. This strength, in turn, is proportional to the sample thickness. Here, the quantum interference phase (Φ_{QI}) is the "real intrinsic" property, which is also confirmed by our experiments.

In the revised manuscript, we have included the introduction and discussion about the intrinsic and extrinsic nature of quantum anisotropy.

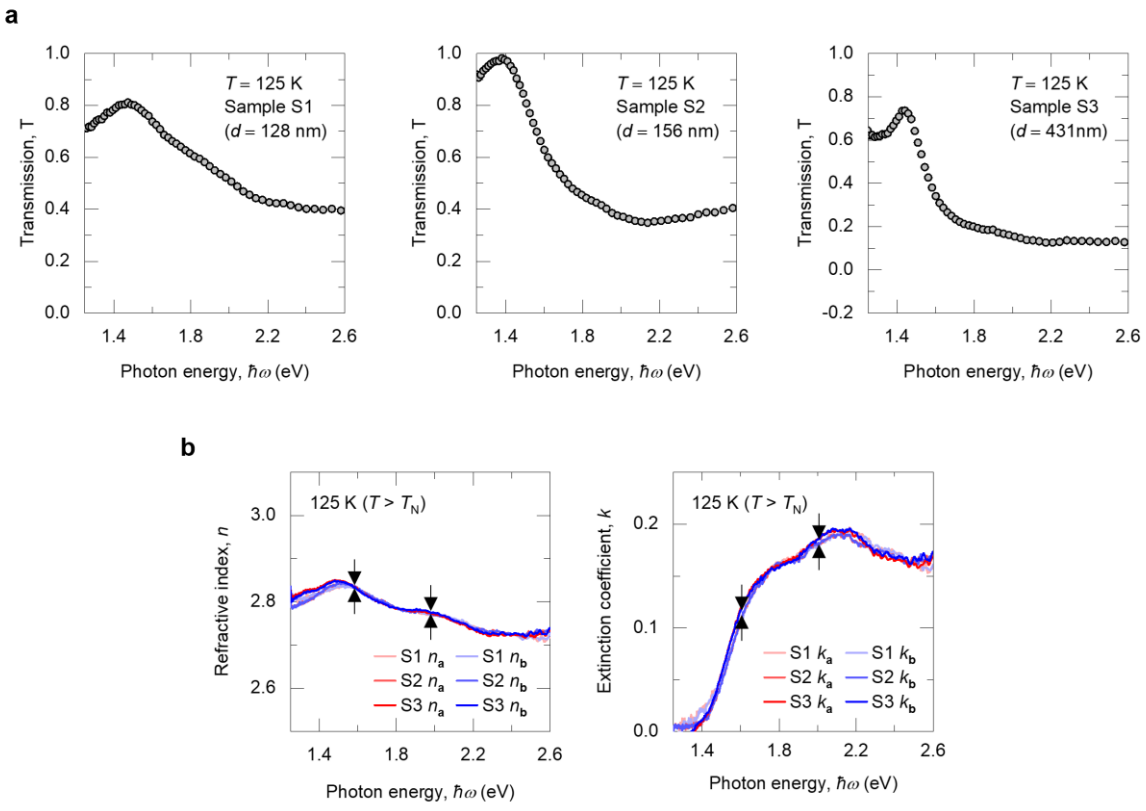

Fig. R1-1 (new Supplementary Fig. S8 in the revised manuscript) | Intrinsic nature of *n* and *k* above T_N, despite the different thickness. a, Raw transmission spectra of three samples with different thicknesses. **b**, Nearly identical *n* and *k* spectra for all three samples, confirming thickness-independent behavior. Negligible variation (indicated by two arrows) appears due to the lack of quantum interference above T_N. (Note: **b** corresponds to Fig. 4**a** in the main text.)

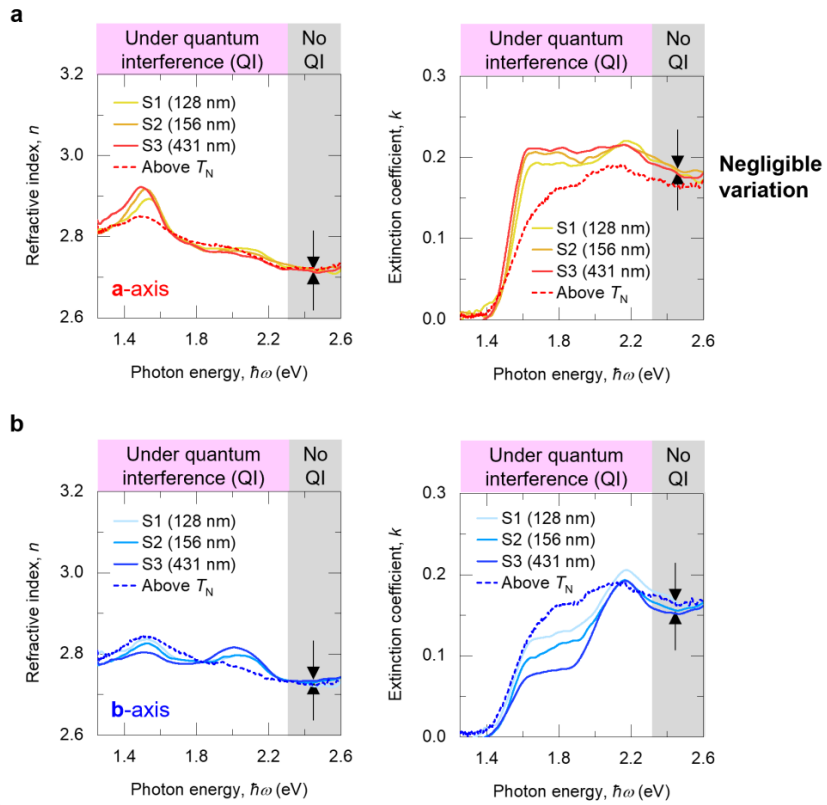

Fig. R1-2 (new Supplementary Fig. S9 in the revised manuscript) | Negligible thickness-dependent variation of *n* and *k* in the spectral region free from quantum interference (QI). a, Along the **a**-axis, *n* and *k* spectra for three samples with different thicknesses. Negligible variation (indicated by two arrows) appears without quantum interference (grey shaded region) whereas large variation emerges under quantum interference (pink shaded region). **b**, Along the **b**-axis, *n* and *k* spectra for three samples with different thicknesses.

Next, we clarify the origin of quantum anisotropy. Although the reviewers did not ask for this, we made an effort to make the work better enough for Nature Communications. For this, we conducted additional light polarization angle-resolved measurements at low temperatures. We concluded that there is quantum interference between anisotropic polarization (below TN) and isotropic background polarization (at all temperatures) (see Fig. R1-3 a-f).

In our case, the AFM ordering below the Néel temperature induces an additional anisotropic polarization, leading to the coexistence of isotropic and anisotropic

polarizations (see Fig. R1-3). This coexistence, characterized by a definite spectral overlap, enables quantum interference between the two coupled channels. Due to their overlapping spectral ranges, quantum interference inevitably occurs between the two excitation channels (in this case, the isotropic polarization and spin-mediated anisotropic polarization), resulting in quantum anisotropy.

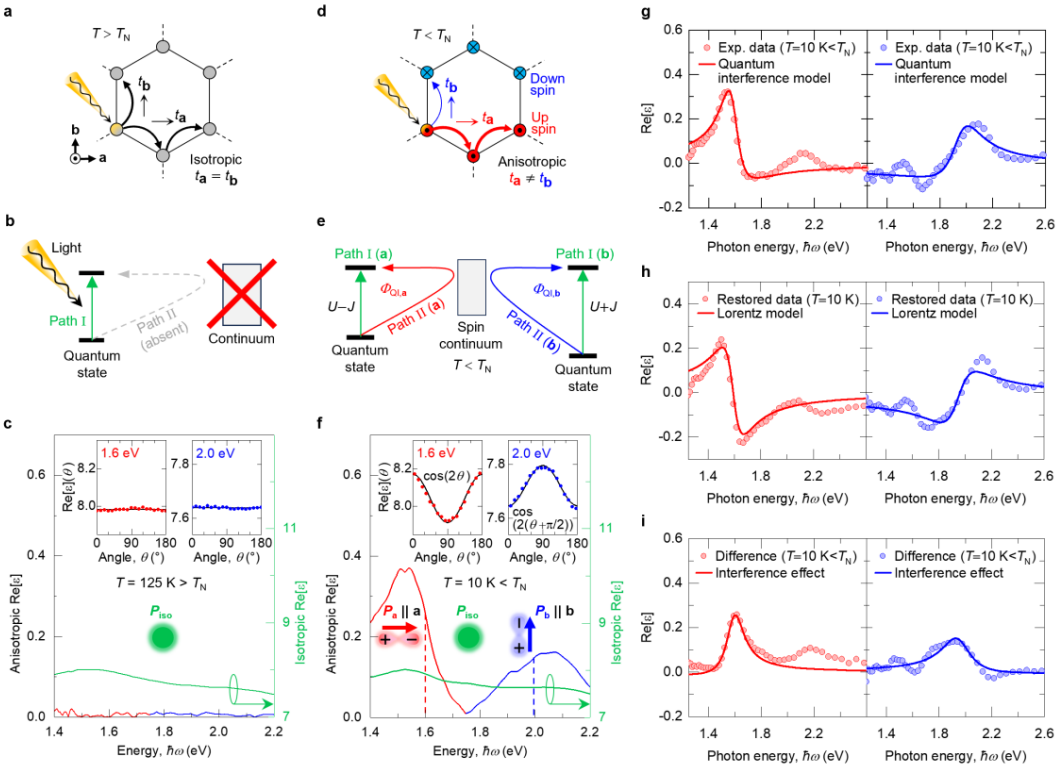

Fig. R1-3 (new Fig. 1 in the revised manuscript) | Light-induced quantum interference in $FePS_3$. a, Above T_N, light-induced dipole transitions (*d-d* transitions) occur between Fe^{2+} ions on the honeycomb lattice. These transitions involve the hopping of electrons between neighboring Fe^{2+} ions, resulting in isotropic optical transitions. The grey balls represent spin-unpolarized Fe^{2+} ions, and the curly arrow indicates light illumination. The symbols ta and tb denote electron hopping along the **a** and **b** directions, respectively. **b**, Above T_N, light-induced dipole transitions occur through a single quantum pathway (Path I, green line). The absence of additional states (continuum) prevents the formation of secondary quantum pathways. **c**, Above T_N, only isotropic polarization is observed (green line and sphere). Anisotropic polarization, indicated by red (**a** direction, ~1.6 eV) and blue (**b** direction, ~2.0 eV) lines, is nearly absent. The angle-dependent polarization data (inset) further confirms the isotropic nature of the polarization at these energies. **d**, Below T_N, light-induced *d-d* transitions become anisotropic. This anisotropy arises from two types of d-d transitions: ta between parallel spins and tb between antiparallel spins. Red and blue balls represent up-spin and down-spin polarized Fe^{2+} ions, respectively. **e**, The presence of two distinct quantum pathways enables quantum interference. A second quantum pathway (Path II) emerges below T_N, coupling to other states and interfering with the original Path I. This interference leads to a phase difference ($\Phi_{QI,a(b)}$) between the two pathways for each direction (**a** and **b**).**f,** Strong anisotropic polarization emerges below T_N, as evidenced by the

cosine-like dispersion in the angle-dependent polarization (inset). The polarization aligns along the **a** direction at 1.6 eV and along the **b** direction at 2.0 eV. **g-i**, Separation of quantum and classical anisotropy. Left (right) panels for **a** (**b**) direction. **(g)** The dielectric constant (the real part proportional to the polarization **P**) measured at T = 10 K < T_N, corresponding to the quantum anisotropy (classical anisotropy + quantum interference effect). **(h)** Restored dielectric constant responsible for classical anisotropy. **(i)** The difference dielectric constant attributed to the quantum interference effect.

At this point, the most crucial point is how large the quantum interference effect is compared to classical anisotropy. If the quantum interference effect is substantially weaker than classical anisotropy, it will not be a significant advancement. The results look striking; the contribution of n and k from the quantum interference is comparable with those of classical anisotropy. Below is their comparison (Fig. R1-4; **a** for classical anisotropy, **b** for quantum anisotropy).

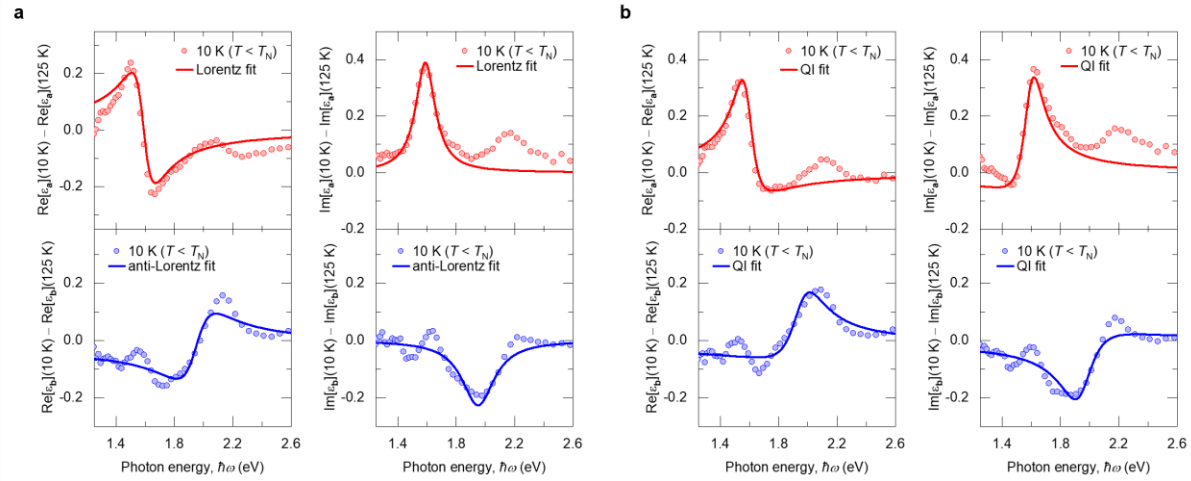

Fig. R1-4 (new Supplementary Fig. S4) | Comparison of quantum anisotropy with classical anisotropy (details of Fig. 1(i)). a, Restored classical anisotropy in the dielectric constant. The classical anisotropy is restored by multiplying exp(-iΦ_{QI}) to (or by removing quantum interference effect from) the experimental ε in **b**. **b**, Quantum anisotropy in the dielectric constant.

Let us discuss the steady-state and ultrafast measurements, in terms of quantum anisotropy. We agree that it is important to distinguish between pump-probe and steady-state measurements. Pump-probe experiments probe non-equilibrium states, where the system's state at time t1 and t2 is described by a single time delay parameter. We propose an alternative approach using light: considering two states at frequencies ω1 and ω2 that are influenced by each other and described by a single interference phase parameter. When a photon is incident, two coupled channels (dipole resonators) can be simultaneously excited, either intrinsically or extrinsically. For simultaneous excitation, the two resonators must have either identical center frequencies or overlapping spectral bandwidths. Under

these conditions, quantum mechanical interference between the two channels can occur.

In this context, we believe that the light-matter interaction, specifically the light-induced quantum mechanical interference is an integral part of the intrinsic properties of the system.

Finally, we need to discuss about physical meaning of the different amplitude of the effects depending on the thickness: the amplitude change proportional to the thickness. In the original manuscript, we proposed “a synergy between quantum interference and thickness”. In the revised manuscript, we provided more detailed explanation, together with experimental evidence (Fig. R1-5). We also included the related text in the revised manuscript as below: (Page 9) “We propose a more realistic explanation for the thickness-dependent n and k values in the quantum interference regime: a synergy between quantum interference and sample thickness. The exotic thickness proportionality of quantum anisotropy may come from the intrinsic quantum interference effect. The magnitude of these effects is directly proportional to the number of dipole moments (i.e., polarizations) involved in the interference process, which scales with sample thickness. Our analysis indicates that the emerging anisotropic polarization below T_N exhibits a similar thickness proportionality, clarifying the relationship between quantum interference and quantum anisotropy (see Supplementary Information S11). In contrast, the Φ_{QI} is a thickness-independent intrinsic property, as confirmed by our experiments (Fig. 5a). Such quantum anisotropy is distinct from both intrinsic classical anisotropy and extrinsic effects like multiple internal reflections, which can be mitigated by varying the sample thickness. The thickness dependence of quantum anisotropy offers an intriguing opportunity to engineer and control the strength of quantum interference effects, enabling the exploration of new phases of matter, from bulk to monolayer limits.”

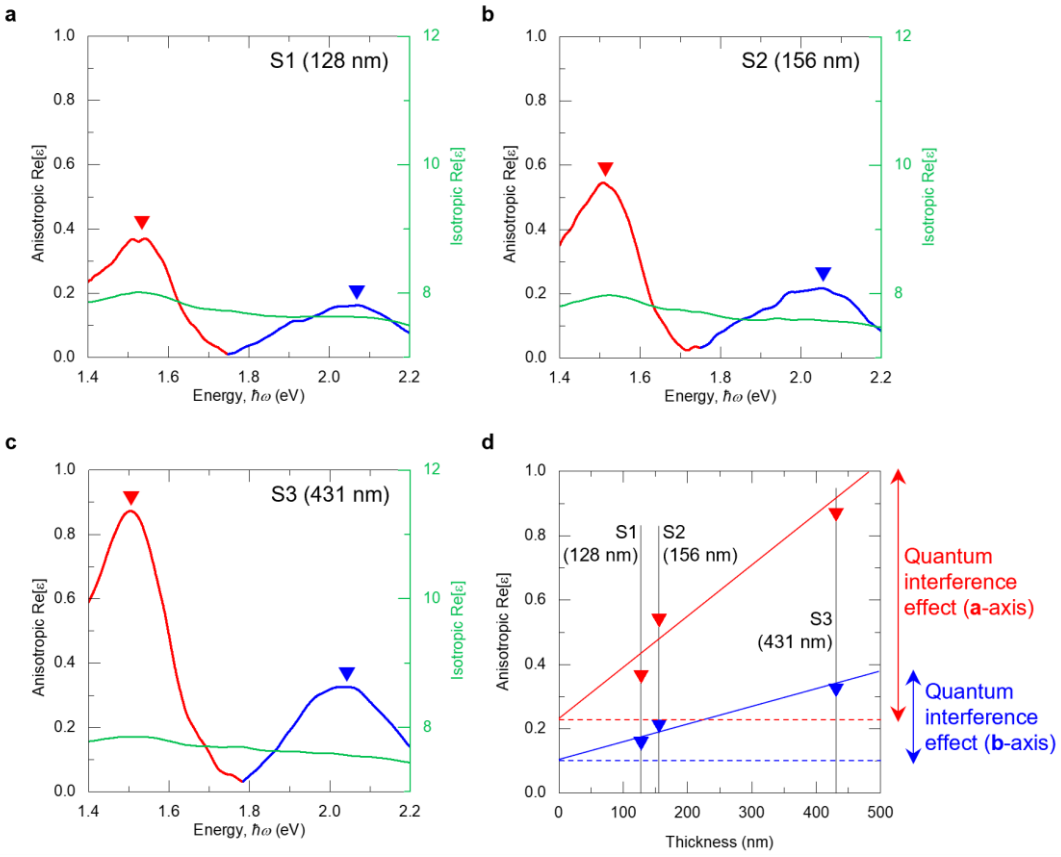

Fig. R1-5 (new supplementary Fig. S11 in the revised manuscript) | Thickness-dependent anisotropic polarization. a-c, Real part of the dielectric constant (Re[ε]) for three samples (S1-S3) with different thicknesses. The red and blue lines represent the anisotropic Re[ε] along the **a** and **b** directions, respectively. The red and blue triangles indicate the peak positions. The green lines represent the isotropic Re[ε], which are nearly identical for all three samples. **d**, Thickness dependence of the anisotropic Re[ε]. The dashed line represents the estimated anisotropic Re[ε] without quantum interference effects, which is expected to be thickness-independent. The solid lines show the linear trend of the anisotropic Re[ε] with quantum interference effects, with red and blue lines corresponding to the **a**-axis and **b**-axis, respectively.

(3) The manuscript writes "We note that the Raman data do not show any change, ruling out the possibility of structural phase transition-induced anisotropy." However, this AFM transition is related the structural distortion as demonstrated in Nature 620, 988-993 (2023) and Nature communication 13, 6598 (2022).

Reply) We agree that this comment is crucial for a comprehensive understanding of both steady-state and non-equilibrium phenomena. We would like to emphasize that our steady-state work and previous non-equilibrium studies are not contradictory.

Previous studies [Nature 620, 988-993 (2023), Nature communication 13, 6598 (2022)], which are wonderful works, have investigated spin-lattice coupling (spin shear stress) on ultrafast timescales. However, the shear stress induced by AFM ordering is transient and has a finite lifetime. In our steady-state measurements, the shear stress does not significantly influence quantum interference due to its limited

duration. We believe that a future study investigating the dynamics of the quantum interference effect and related phase transitions using pump-probe spectroscopy would be highly valuable. We would be interested in collaborating on such a project. Thank you for your suggestion.

Small suggestions

(4) I have some small suggestions on the introduction part. The author may want to generalize this quantum interference from linear optics to non-linear optics, such as second harmonic generation (SHG). There may be a few contributions (magnetic and electric dipole) to SHG and these contributions can have interference and give rise a quantum phase, for example in Nature materials 23, 790–795 (2024), where an electronic polarization is induced by light.

Reply) We thank you for your insightful comment. We appreciate your feedback, as it has helped us identify an important aspect of our work that we had not previously considered. In response, we have revised the introduction to include a discussion of both linear and nonlinear optical phenomena.

We were happy to expand the introduction (as below) to include both linear and nonlinear optics, as suggested. Thank you for your valuable feedback.

(Page 3) “This quantum interference could be further generalized to non-linear optics, where the ultrafast external fields couple to electronic order parameters, potentially leading to quantum interference between electric and magnetic dipoles [23].” before “Here, we …”.

(5) The manuscript presents 6 figures in total and only 3 of them are experimental data. The authors may put 1-2 into Supplementary material to shorten the length.

Reply) We think this comment is very beneficial for making the manuscript easier to read. The original Figs. 1 and 2 (theory or analysis portions) were moved to the Supplementary Figs. 3 and 4 with the relevant texts (Supplementary Notes) in the revised manuscript, in response to the comment. Additionally, we created a new Fig. 1 (based on direct experimental data) as a replacement that directly shows the origin of quantum interference and related quantum anisotropy (Please see our replies to (2) and (3)).

% Further revisions:

1) Revised introduction (page 2-3)
2) Revised description of new Fig. 1 (page 4-5)
3) Revised interpretation & discussion (page 8-9)
4) Revised and included figures below:

4-1) Assignment of anisotropic polarizations

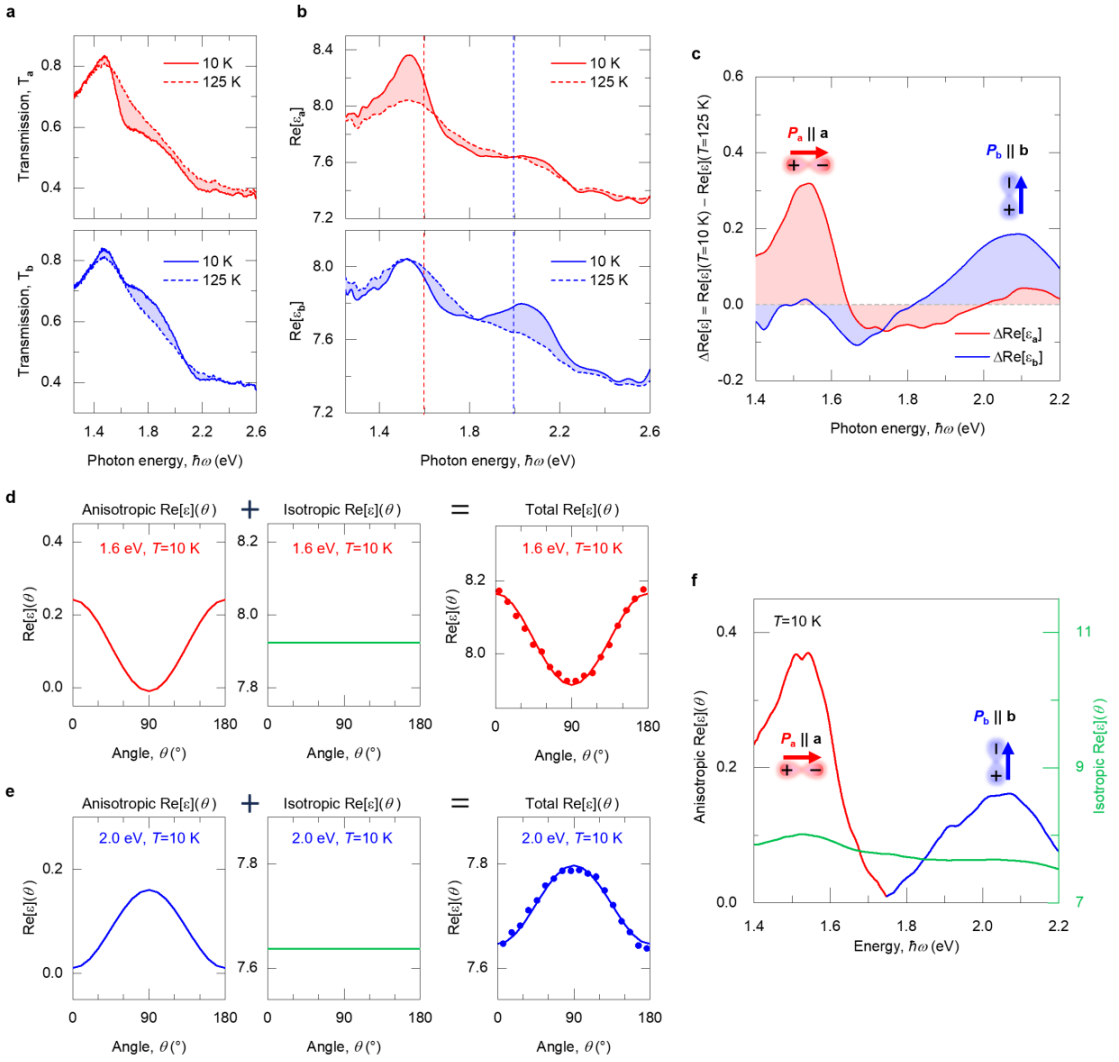

Supplementary Fig. S1 | Assignment of anisotropic polarizations: $P_{a(b)}$ in the a(b) direction. a, Raw transmission spectra at T = 10 K (solid lines) and T = 125 K (dashed lines) for light polarized along the **a** and **b** directions. **b**, Calculated dielectric constant at 10 K and 125 K for light polarized along the a and b directions. Re denotes the real part. **c**, Dielectric constant difference (ΔRe[ε] = Re[ε] (10 K) - Re[ε] (125 K)): along the **a** direction (red line) and along the **b** direction (blue line). The emergence of $\mathbf{P_a}$ and $\mathbf{P_b}$ is schematically illustrated below. **d**,**e**, Angle-resolved dielectric constant at 10 K for 1.6 eV (**d**) and 2.0 eV (**e**). The total dielectric constant (right panels) is a superposition of isotropic (middle panels) and anisotropic polarizations (left panels). The anisotropic polarization at 2.0 eV is out of phased to that at 1.6 eV. **f**, Energy dependence of anisotropic (red and blue lines) and isotropic (green line) polarizations.

4-2) More clear description for the d-d transition

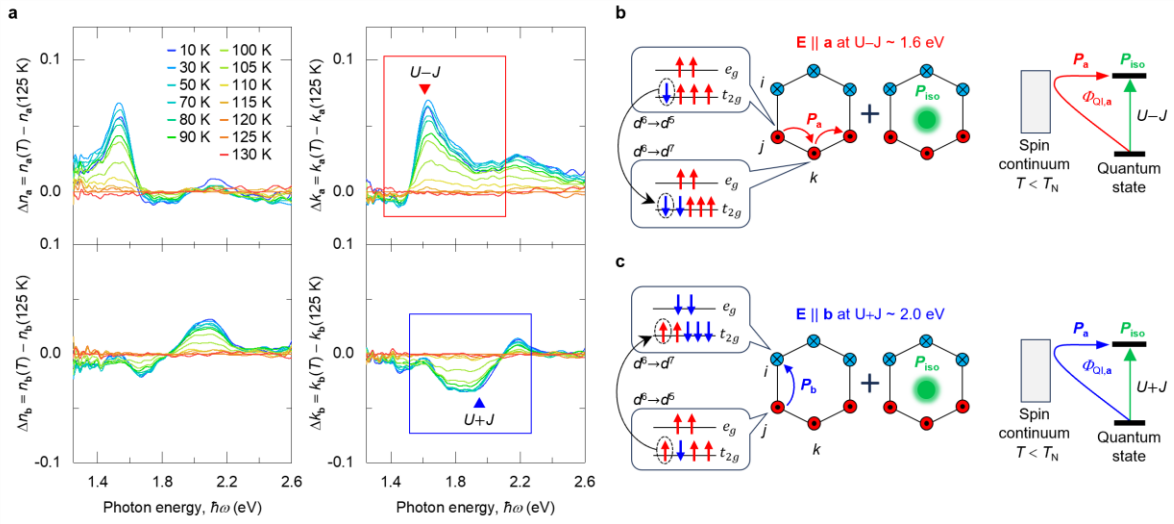

Figure 2 | Experimental demonstration of quantum anisotropy in $FePS_3$. **a**, The change in the refractive index (*n* and *k*) as a function of temperature. (Left panels) $\triangle n = n\,(T) - n\,(T = 125\ \mathrm{K})$ in both **a** and **b** directions. (Right panels) $\triangle k = k\,(T) - k\,(T = 125\ \mathrm{K})$ in both **a** and **b** directions. Subscripts a and b indicate the **a** and **b** direction, respectively. The center frequencies of the $\triangle k$ peaks (inside the box) correspond to the *d*-*d* transition energies U–J ≈ 1.6 eV (**a** direction) and U+J ≈ 2.0 eV (**b** direction) below T_N. **b**, Schematic illustration of the light-induced electron hopping between Fe^{2+} ions along the **a**-direction occurs at U–J ≈ 1.6 eV resulting in the $\mathbf{P}_a$, in conjunction with the background $\mathbf{P}_{iso}$ (left schematic). The initial ground state consists of two Fe^{2+} ions with a d^6 configuration (six electrons in the *d* orbitals), while the excited state involves one Fe^{2+} ion with a d^5 configuration and another with a d^7 configuration. The curved black arrow indicates the light-induced transfer of a spin-up electron (dashed circles). The orbital configuration, including the e_g and t_{2g} orbitals, is determined by Coulomb repulsion (U) and Hund's exchange energy (J). The $\mathbf{P}_a$ and $\mathbf{P}_{iso}$ polarizations undergo quantum mechanical interference (right schematic). **c**, Schematic illustration of the light-induced electron hopping between Fe^{2+} ions along the **b**-direction occurs at U+J ~ 2.0 eV (left schematic). The $\mathbf{P}_b$ and $\mathbf{P}_{iso}$ polarizations undergo quantum mechanical interference (right schematic).

4-3) Reliability of the data by comparing both new (low-k approximation) and old (model fitting) methods.

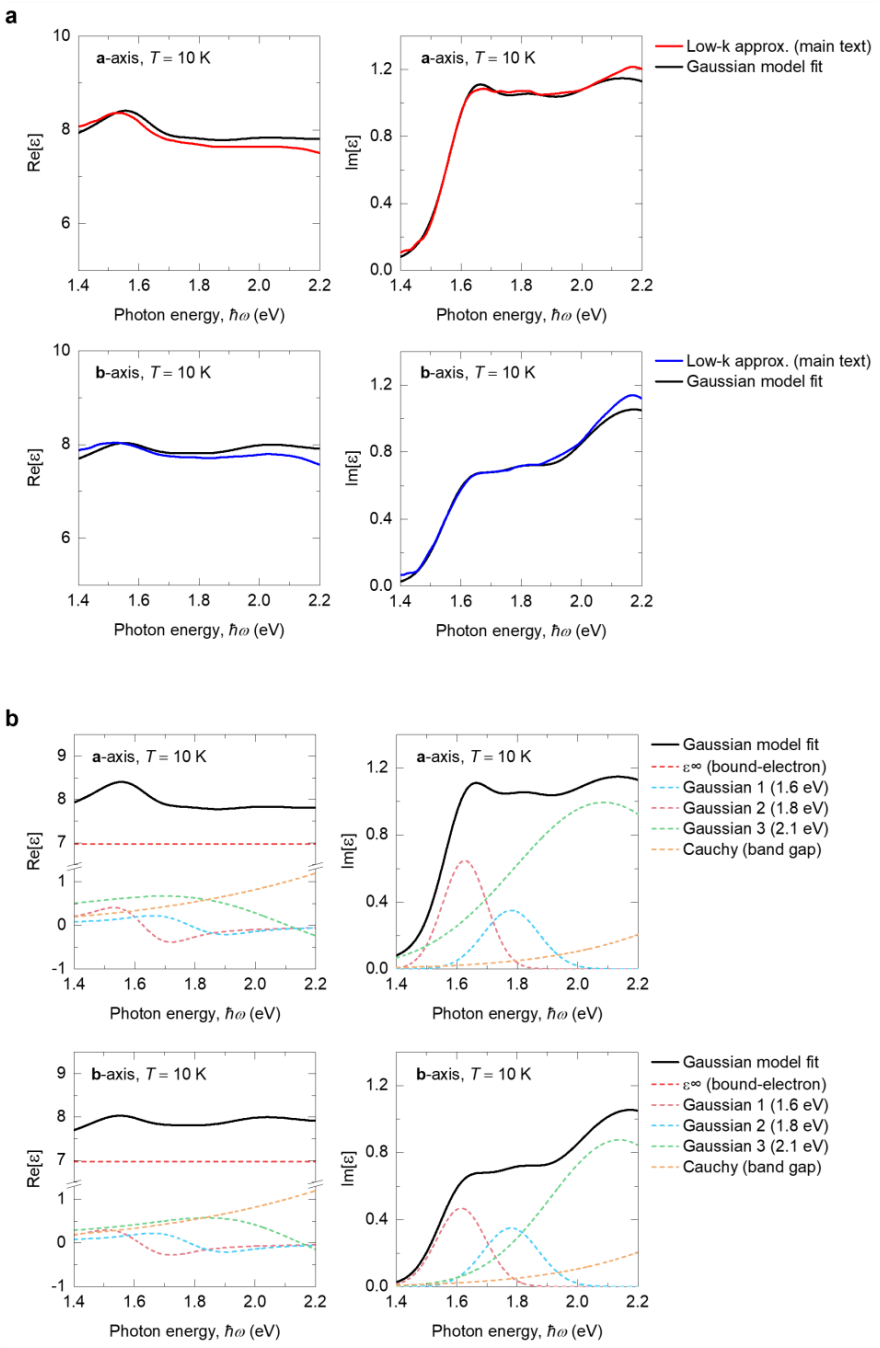

Supplementary Fig. S6 | Calculation of complex dielectric constant of a, b axes at 10 K. a, Comparison of dielectric constants obtained through two different approaches: i) Low-k approximation used for the results in the mains text and ii) Gaussian fitting for comparison. Real part (left) and imaginary part (right) of the dielectric constant for the **a** direction (top) and the **b** direction (bottom). **b**, Details of optical constants model fitting, which is composed of three Gaussian models and one Cauchy model.

Reviewer #2 (Remarks to the Author):

This study investigates light-matter interaction induced quantum anisotropy in van der Waals (vdW) antiferromagnetic (AFM) semiconductors, particularly FePS3, focusing on the quantum interference between light-induced quantum pathways. The interaction causes spontaneous symmetry breaking of dipole moments and leads to phenomena such as birefringence and linear dichroism below the Néel temperature. While the manuscript offers valuable insights, several revisions and clarifications are necessary before publication.

Reply) We could tell the reviewer was knowledgeable and had put a lot of effort into the review from all of the comments. To show our respect, we revised the manuscript based on the valuable comments. Our manuscript has been refined to be appropriate for publication in Nature Communications, as a result of the feedback. We are convinced that this type of author-reviewer collaboration results in significant scientific advancement.

We appreciate your concern regarding the intrinsic nature of n and k. As you correctly pointed out, the anisotropic n and k observed in $FePS_3$ below TN arise from classical anisotropy due to AFM spin ordering. However, the quantum anisotropy we report is distinct from this classical effect. Quantum anisotropy leads to a thickness-dependent behavior of n and k, unlike the intrinsic nature of n and k in the absence of quantum interference.

To clarify this distinction, we have provided the following evidence:

1. **Intrinsic Behavior Above TN:** We demonstrate that n and k are thickness-independent above TN for all three samples.
2. **Quantum Interference Regime:** We identify a spectral region where quantum interference leads to thickness-dependent n and k.
3. **Classical Regime:** We show that outside the quantum interference region (below 1.4 eV and above 2.4 eV), n and k remain thickness-independent, exhibiting classical behavior.

For a detailed discussion, please refer to our responses to comments #1– #4.

To address the issues raised in #5 – #7, we also clarified a major misunderstanding regarding the model fitting. **In the revised manuscript, we introduced two methods: I) low-k approximation without resorting model fitting (main text and Methods), in comparison with ii) model fitting (supplementary)** with three oscillators that have a clear physical meaning**. Their consistency significantly enhances the reliability of our data and analysis.**

1. The emerging of birefringence and linear dichroism in FePS3 is already known due to spin-charge coupling in AFM semiconductors (Nano Lett. 21, 6938−6945 (2021), Nature Photonics 16, no. 4, 311-317 (2022)). The authors need to better articulate the significance of observing quantum interference and, consequently, LB and LD in FePS3 crystal.

2. The authors mention "quantum interference, which is further enhanced by the thickness effect," on page 2, line 12. Figure 5 shows the difference in linear birefringence (LB) and linear dichroism (LD) depending on the thickness. However, the authors should explain what types of enhancement can be observed. Is it just an increased value of LB and LD? If the crystal's thickness increases to bulk or decreases to a monolayer, is it possible to observe more increased or decreased values of LB and LD? Furthermore, it is unconventional to observe a significant difference in refractive index depending on the thickness of the material. The authors proposed "a synergy between quantum interference and thickness". However, the authors should provide more evidence of the enhancement caused by longer optical path-induced quantum interference.

3. The refractive index and extinction coefficient are functions of wavelength, and it is conventional to report the LB and LD values as a function of wavelength. (Nat. Photonics 12, 392−396 (2018), Nature Communications volum, 12, Article number: 854 (2021)). According to the definition of quantum anisotropy in this paper, all other birefringent crystals should exhibit quantum anisotropy. The authors should clarify the definitions of conventional and quantum anisotropy.

Reply) We believe this comment is crucial and acknowledge that there may have been a misunderstanding. We apologize for the confusion. We will address comments #1 − #3 simultaneously in the following response.

We agree with your comment on classical anisotropy "The emerging of birefringence and linear dichroism in FePS3 is already known due to spin-charge coupling in AFM semiconductors". We are going to clarify the difference between classical anisotropy (linear birefringence and linear dichroism) and quantum anisotropy.

To clarify this distinction, we have provided the following direct evidence:

1. Intrinsic Behavior Above TN (Fig. R2-1): We demonstrate that n and k are thickness-independent above TN for all three samples.

First, we would like to clarify that we have accurately measured and considered the thickness of each sample in our calculations of n and k.

2. Quantum Interference Regime Below TN (Fig. R2-2): We identify a spectral region where quantum interference leads to thickness-dependent n and k.

3. Classical Regime Below TN (Fig. R2-2): We show that outside the quantum interference region (above 2.4 eV, below 1.4 eV, unfortunately, the data quality is compromised due to limitations in our spectrometer's bandwidth.), n and k remain thickness-independent, exhibiting classical behavior.

Additionally, we have investigated the thickness dependence of n and k, which is a key finding that directly reflects the quantum interference effect. To directly address this issue, we present the full range of n and k spectra, which exhibit two distinct regions: with and without quantum interference (Fig. R2-2). **In the absence of quantum interference, as you correctly pointed out, the n and k spectra are identical for all sample thicknesses.** However, in the quantum interference region, the n and k spectra vary significantly across different thicknesses. [Importantly, the quantum interference phase Φ_{QI} remains independent of thickness, showing its "real intrinsic" nature.] While the importance of intrinsic properties is widely recognized, the role of Φ_{QI} has been often overlooked in various fields of physics. This work underscores the significance of Φ_{QI} in fundamental physics.

We note that quantum anisotropy seems to be both intrinsic and extrinsic.

1) Intrinsic nature: When a photon is incident, two channels (dipole resonators) with their spectral overlap are simultaneously excited and therefore their quantum interference is inevitable, which seems to be intrinsic.
2) Extrinsic nature: As we have shown that quantum LB and LD are proportional to the sample thickness, quantum LB and LD are thickness-dependent like extrinsic properties. Nevertheless, quantum LB and LD are also distinct from purely extrinsic effects like multiple internal reflections that can be avoided by changing the thickness of the sample.

Such exotic nature of quantum LB and LD arises from the intrinsic character of the quantum interference effect. Their magnitude depends on the number of dipole moments (which is proportional to the thickness) involved in the quantum interference process. This strength, in turn, is proportional to the sample thickness. Here, the quantum interference phase (Φ_{QI}) is the "real intrinsic" property, which is also confirmed by our experiments.

In the revised manuscript, we have included the introduction and discussion about the intrinsic and extrinsic nature of quantum anisotropy.

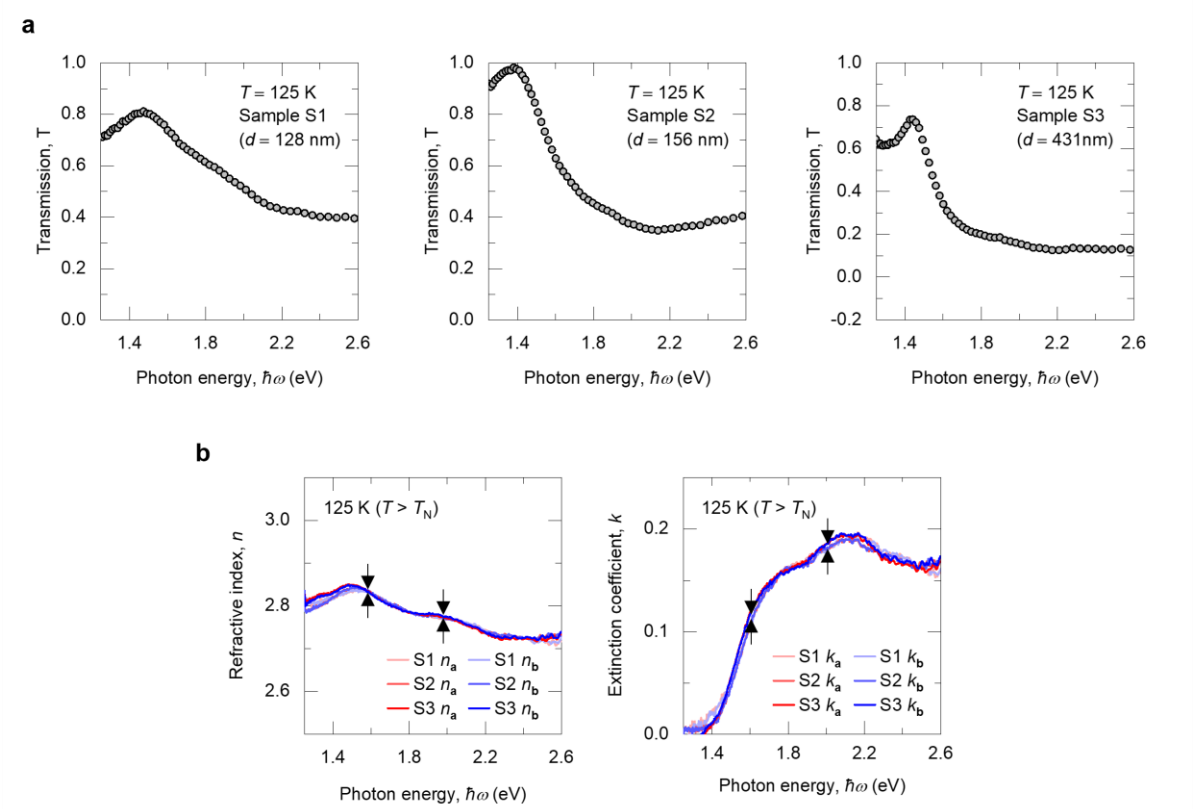

Fig. R2-1 (new Supplementary Fig. S8 in the revised manuscript) | Intrinsic nature of *n* and *k* above T_N, despite the different thickness. a, Raw transmission spectra of three samples with different thicknesses. **b**, Nearly identical *n* and *k* spectra for all three samples, confirming thickness-independent behavior. Negligible variation (indicated by two arrows) appears due to the lack of quantum interference above T_N. (Note: **b** corresponds to Fig. 4**a** in the main text.)

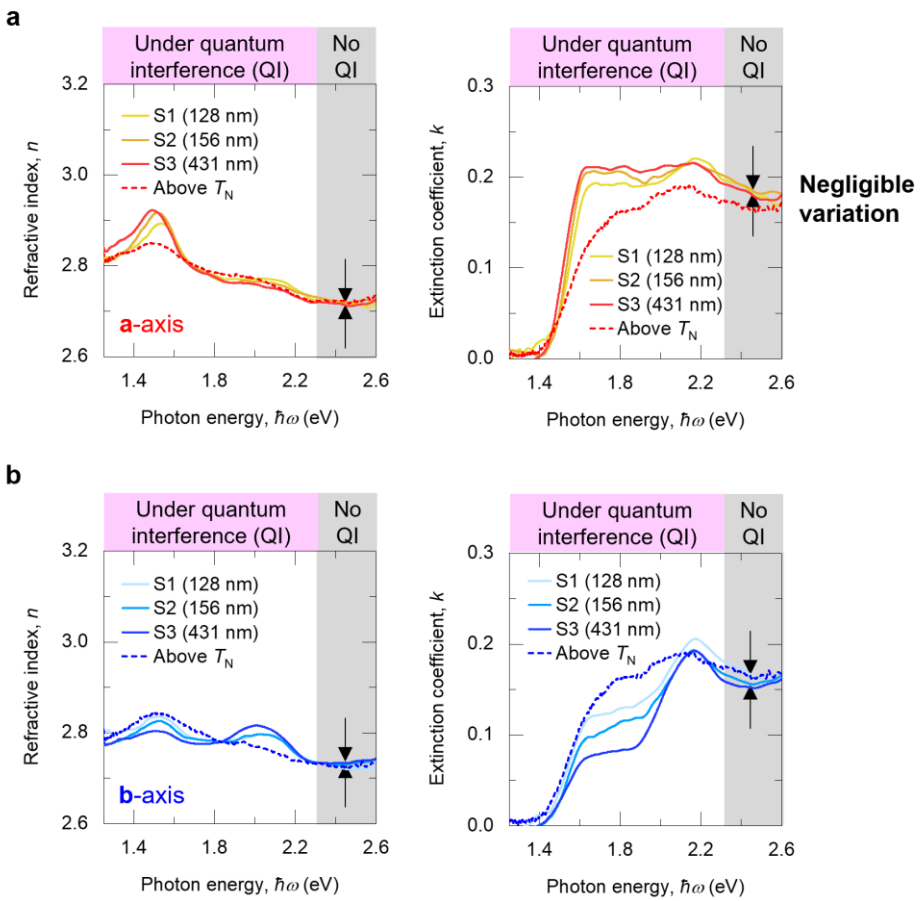

Fig. R2-2 (new Supplementary Fig. S9 in the revised manuscript) | Negligible thickness-dependent variation of *n* and *k* in the spectral region free from quantum interference (QI). **a**, Along the **a**-axis, *n* and *k* spectra for three samples with different thicknesses. Negligible variation (indicated by two arrows) appears without quantum interference (grey shaded region) whereas large variation emerges under quantum interference (pink shaded region). **b**, Along the **b**-axis, *n* and *k* spectra for three samples with different thicknesses.

Next, we clarify the origin of quantum anisotropy. Although the reviewers did not ask for this, we made an effort to make the work better enough for Nature Communications. For this, we conducted additional light polarization angle-resolved measurements at low temperatures. We concluded that there is quantum interference between anisotropic polarization (below TN) and isotropic background polarization (at all temperatures) (see Fig. R2-3 a-f).

In our case, the AFM ordering below the Néel temperature induces an additional anisotropic polarization, leading to the coexistence of isotropic and anisotropic polarizations (see Fig. R2-3). This coexistence, characterized by a definite spectral overlap, enables quantum interference between the two coupled channels. Due to their overlapping spectral ranges, quantum interference inevitably occurs between the two excitation channels (in this case, the isotropic polarization and spin-mediated anisotropic polarization), resulting in quantum anisotropy.

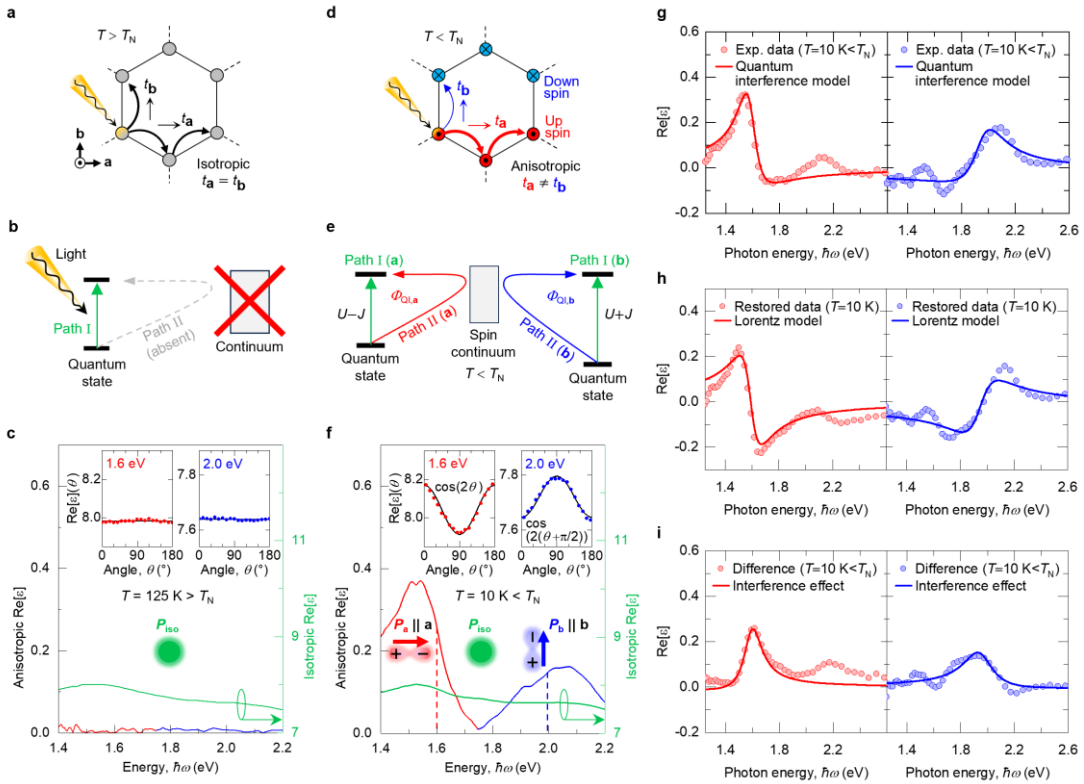

Fig. R2-3 (new Fig. 1 in the revised manuscript) | Light-induced quantum interference in $FePS_3$. a, Above T_N, light-induced dipole transitions (*d-d* transitions) occur between Fe^{2+} ions on the honeycomb lattice. These transitions involve the hopping of electrons between neighboring Fe^{2+} ions, resulting in isotropic optical transitions. The grey balls represent spin-unpolarized Fe^{2+} ions, and the curly arrow indicates light illumination. The symbols ta and tb denote electron hopping along the **a** and **b** directions, respectively. **b**, Above T_N, light-induced dipole transitions occur through a single quantum pathway (Path I, green line). The absence of additional states (continuum) prevents the formation of secondary quantum pathways. **c**, Above T_N, only isotropic polarization is observed (green line and sphere). Anisotropic polarization, indicated by red (**a** direction, ~1.6 eV) and blue (**b** direction, ~2.0 eV) lines, is nearly absent. The angle-dependent polarization data (inset) further confirms the isotropic nature of the polarization at these energies. **d**, Below T_N, light-induced *d-d* transitions become anisotropic. This anisotropy arises from two types of d-d transitions: ta between parallel spins and tb between antiparallel spins. Red and blue balls represent up-spin and down-spin polarized Fe^{2+} ions, respectively. **e**, The presence of two distinct quantum pathways enables quantum interference. A second quantum pathway (Path II) emerges below T_N, coupling to other states and interfering with the original Path I. This interference leads to a phase difference ($\Phi_{QI,a(b)}$) between the two pathways for each direction (**a** and **b**).**f,** Strong anisotropic polarization emerges below T_N, as evidenced by the cosine-like dispersion in the angle-dependent polarization (inset). The polarization aligns along the **a** direction at 1.6 eV and along the **b** direction at 2.0 eV. **g-i**, Separation of quantum and classical anisotropy. Left (right) panels for **a** (**b**) direction. **(g)** The dielectric constant (the real part proportional to the polarization **P**) measured at T = 10 K < T_N, corresponding to the quantum anisotropy (classical anisotropy + quantum interference effect). **(h)** Restored dielectric constant responsible for classical anisotropy. **(i)** The difference dielectric constant attributed to the quantum interference effect.

At this point, the most crucial point is how large the quantum interference effect is compared to classical anisotropy. If the quantum interference effect is substantially weaker than classical anisotropy, it will not be a significant advancement. The results look striking; the contribution of n and k from the quantum interference is comparable with those of classical anisotropy. Below is their comparison (Fig. R2-4; **a** for classical anisotropy, **b** for quantum anisotropy).

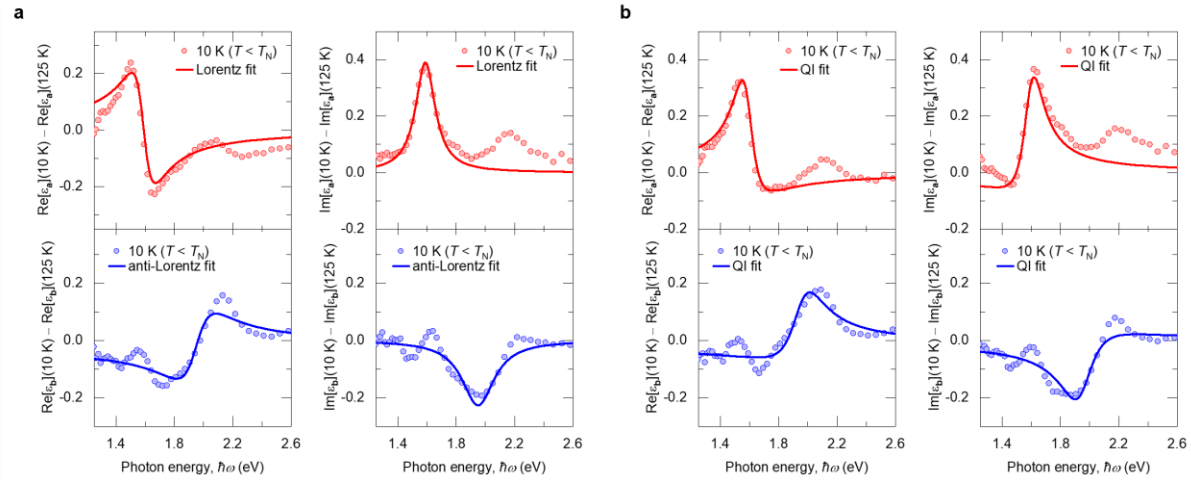

Fig. R2-4 (new Supplementary Fig. S4) | Comparison of quantum anisotropy with classical anisotropy (details of Fig. 1(i)). a, Restored classical anisotropy in the dielectric constant. The classical anisotropy is restored by multiplying $\exp(-i\Phi_{QI})$ to (or by removing quantum interference effect from) the experimental ε in **b**. **b**, Quantum anisotropy in the dielectric constant.

Finally, we need to discuss about physical meaning of the different amplitude of the effects depending on the thickness: the amplitude change proportional to the thickness. In the original manuscript, we proposed "a synergy between quantum interference and thickness". In the revised manuscript, we provided more detailed explanation, together with experimental evidence (Fig. R2-5). We also included the related text in the revised manuscript as below: (Page 9) "We propose a more realistic explanation for the thickness-dependent *n* and *k* values in the quantum interference regime: a synergy between quantum interference and sample thickness. The exotic thickness proportionality of quantum anisotropy may come from the intrinsic quantum interference effect. The magnitude of these effects is directly proportional to the number of dipole moments (i.e., polarizations) involved in the interference process, which scales with sample thickness. Our analysis indicates that the emerging anisotropic polarization below T_N exhibits a similar thickness proportionality, clarifying the relationship between quantum interference and quantum anisotropy (see Supplementary Information S11). In contrast, the Φ_{QI} is a thickness-independent intrinsic property, as confirmed by our experiments (Fig. 5a). Such quantum anisotropy is distinct from both intrinsic classical anisotropy and extrinsic effects like multiple internal reflections, which can be mitigated by varying the sample thickness. The thickness dependence of quantum anisotropy offers an intriguing opportunity to engineer and control the strength of quantum interference

effects, enabling the exploration of new phases of matter, from bulk to monolayer limits."

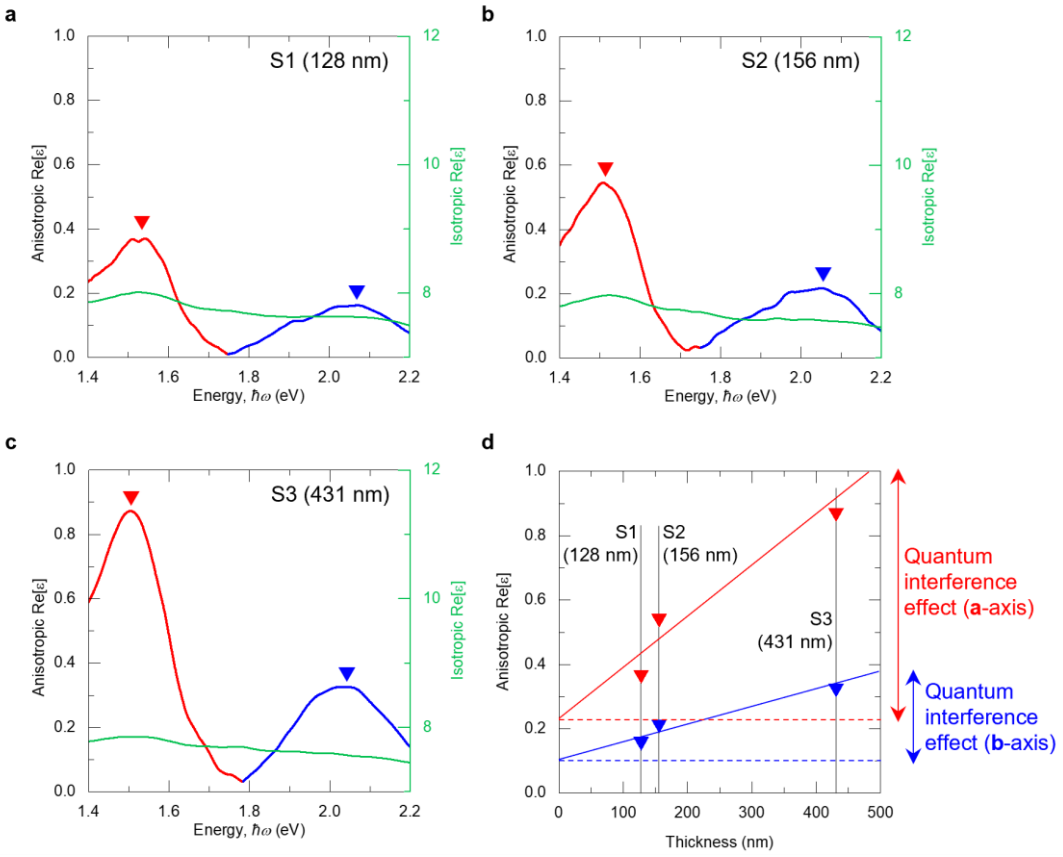

Fig. R2-5 (new supplementary Fig. S11 in the revised manuscript) | Thickness-dependent anisotropic polarization. a-c, Real part of the dielectric constant (Re[ε]) for three samples (S1-S3) with different thicknesses. The red and blue lines represent the anisotropic Re[ε] along the **a** and **b** directions, respectively. The red and blue triangles indicate the peak positions. The green lines represent the isotropic Re[ε], which are nearly identical for all three samples. **d**, Thickness dependence of the anisotropic Re[ε]. The dashed line represents the estimated anisotropic Re[ε] without quantum interference effects, which is expected to be thickness-independent. The solid lines show the linear trend of the anisotropic Re[ε] with quantum interference effects, with red and blue lines corresponding to the **a**-axis and **b**-axis, respectively.

Also, according to the reviewer's comment, we articulate the significance of of observing quantum interference and, consequently, LB and LD in the revised manuscript (three paragraphs).

(I) Introduction (page 2-3): "However, the understanding of "quantum-mechanical" light-matter interaction remains incomplete. The key aspect is that photons provide a phase to complex quantities of matter, such as refractive index through quantum interference, leading to the phase-induced symmetry breaking of materials. When a photon is incident, two coupled channels (two dipole resonators) can be simultaneously excited, either intrinsically or extrinsically. For simultaneous

excitation, the two resonators must have either identical center frequencies or overlapping spectral bandwidths, with one being sharp and the other broad. Under these conditions, the two channels can interfere quantum mechanically. In van der Waals (vdW) hexagonal antiferromagnetic (AFM) semiconductor $FePS_3$, the conventional (or classical) linear birefringence (LB) and linear dichroism (LD) are well-known to arise from spin-charge coupling below the Néel temperature T_N[20,21]. The classical anisotropy is also related to the emergent anisotropic dipolar polarization below T_N on an isotropic background polarization according to a recent study[22]. Despite the coexistence of two polarizations, however, the potential for their quantum interference has not been previously explored. Importantly, this quantum interference induces a symmetry breaking of the electronic dipole moments (or polarization **P**), giving rise to additional LB and LD, i.e., quantum anisotropy. This quantum interference-induced effect could provide a route towards quantum phase transitions, which has not been considered carefully yet. This quantum interference effect could be further generalized to non-linear optics, where the ultrafast external fields couple to electronic order parameters, potentially leading to quantum interference between electric and magnetic dipoles[23]."

(II) Results (page 5): "We have several important points to highlight regarding quantum anisotropy. Firstly, quantum anisotropy does not necessitate an anisotropic initial state like $FePS_3$ below T_N (see Supplementary Information S2 and S3 for theoretical details). Even in isotropic systems, quantum interference can arise between two spectrally overlapping optical polarizations. Secondly, while directional polarizations, as observed in $FePS_3$ at 1.6 eV (**a**-axis) and 2.0 eV (**b**-axis), facilitate the study of quantum anisotropy, they are not strictly necessary. Quantum anisotropy can emerge from the interplay between two polarizations within a single direction (see Supplementary Information S2 and S3 for theoretical details).. However, the presence of anisotropy, as in $FePS_3$, offers several advantages. It allows us to explore distinct energy-dependent quantum phase transitions at 1.6 eV and 2.0 eV along the **a** and **b** directions, respectively. Additionally, it enables the investigation of quantum mechanical entanglement between the two polarizations, which can be manifested as a sum rule constraint, highlighting the collaboration between optics and quantum mechanics. While isolating pure quantum anisotropy from classical anisotropy can be challenging in $FePS_3$, the benefits of studying quantum anisotropy in this system outweigh this limitation."

(III) Results (page 9): "We propose a more realistic explanation for the thickness-dependent n and k values in the quantum interference regime: a synergy between quantum interference and sample thickness. The exotic thickness proportionality of quantum anisotropy may come from the intrinsic quantum interference effect. The magnitude of these effects is directly proportional to the number of dipole moments (i.e., polarizations) involved in the interference process, which scales with sample thickness. Our analysis indicates that the emerging anisotropic polarization below T_N exhibits a similar thickness proportionality, clarifying the relationship between quantum interference and quantum anisotropy (see Supplementary Information S11). In contrast, the Φ_{QI} is a thickness-independent intrinsic property,

as confirmed by our experiments (Fig. 5a). Such quantum anisotropy is distinct from both intrinsic classical anisotropy and extrinsic effects like multiple internal reflections, which can be mitigated by varying the sample thickness. The thickness dependence of quantum anisotropy offers an intriguing opportunity to engineer and control the strength of quantum interference effects, enabling the exploration of new phases of matter, from bulk to monolayer limits."

4. Is it fair to assume that path1 and path2 have the same resonance frequency with only the phase difference of two electric dipoles, and simplify the model on page 4, lines 23-24? What is the evidence that both path 1 and path 2 have the same resonance frequency?

Reply) We appreciate your valuable comment. The assumption that both path 1 and path 2 have the same resonance frequency is a somewhat strict requirement for quantum interference. As you might think, finite spectral linewidths (characterized by a broadening factor Γ) allow for quantum interference between resonances with slightly different center frequencies. The key requirement is sufficient spectral overlap between the two resonances.

To introduce the importance of the spectral weight, we reconstructed the paragraph in Page 4: "Although light does not directly couple to spin, it interacts with electronic polarization associated with *d*-*d* transitions. The Ising-type spin ordering in $FePS_3$ induces anisotropy in this electronic polarization. Therefore, below T_N, two optical excitation channels coexist: one for isotropic polarization and the other for anisotropic polarization within the spectral region of interest. We experimentally confirm the presence of significant anisotropic polarization near 1.6 eV and 2.0 eV through angle-resolved optical measurements, as shown in Fig. 1f (see Supplementary Information S1 for the detailed assignment of anisotropic polarizations). Because of the spectral overlap between isotropic and anisotropic optical polarizations, their quantum interference naturally arises, leading to quantum anisotropy."

5. The authors need to articulate the adequacy of using only one Lorentz oscillator model to describe this system's quantum interference. As shown in Figures 3a and 5a, multiple oscillations can be observed in the experimental data, particularly at low temperatures. In this regard, the authors should consider the possibility that a simplified model is the reason for the observed deviation from the Lorentzian shape in the $\triangle$n and $\triangle$k lineshapes below the Néel temperature, as mentioned on page 6, lines 14-15. What if the authors use multiple Lorentz oscillators for modeling? Can they observe multiple Lorentzian shapes below the Néel temperature?

6. The authors should provide more detail about obtaining of n, k value. The authors used six oscillators to describe the dielectric function of the material, which is contradictory to using only one Lorentz oscillator for modeling the quantum interference.

Reply) We agree with your concern regarding the fitting procedure, which is a common challenge in spectroscopic analysis. In the revised manuscript, we did not use the model fitting but employ low-k approximation (**Methods**) and modified all the data. But we emphasize that the fitting results in the original manuscript and our new low-k approximation method provide nearly the same results. We will address comments #1 – #3 simultaneously in the following response.

Note that in the original manuscript, the number of oscillators varied between the main text (two oscillators, one for each quantum interference peak at 1.6 eV and 2.0 eV, as you mentioned) and the supplementary materials (six oscillators for precise data conversion from transmission to optical constants, as you mentioned). While our intent was to simplify the explanation in the original manuscript, we acknowledge that the inconsistency may have caused confusion. Sorry about that.

We completely removed such confusion in the revised manuscript. We employed two methods I) low-k approximation (Fig. R2-6) and II) optical constant model fitting (supplementary). For both approaches, the obtained optical constants are consistent (Fig. R2-7**a**). In the main manuscript, we made changes to all of the data obtained using the low-k approximation. We also contrasted this with the model fitting results shown in the Supplementary section (Fig. R-7**b**) to assess the data's reliability. [*We also confirmed the consistency of n and k with those exactly obtained from both transmission and reflection measurements.*]

For the model fitting, in the revised manuscript, we have consistently used three major oscillators centered at around 1.6 eV, 1.8 eV, and 2.0 eV, which can be physically explained with the known d-d transitions in $FePS_3$. This simplification has minimal impact on our results and conclusions. As shown in Fig. R2-8, anisotropic polarization is absent at 1.8 eV, indicating that the oscillator centered at this energy does not contribute to quantum interference. An increase in spectral weight results from the oscillator at 1.6 eV, which consists of both isotropic and anisotropic components and is essential to the quantum interference process. The oscillator at 2.0 eV, which is made up of both isotropic and anisotropic components, also contributes to quantum interference, which lowers the spectral weight.

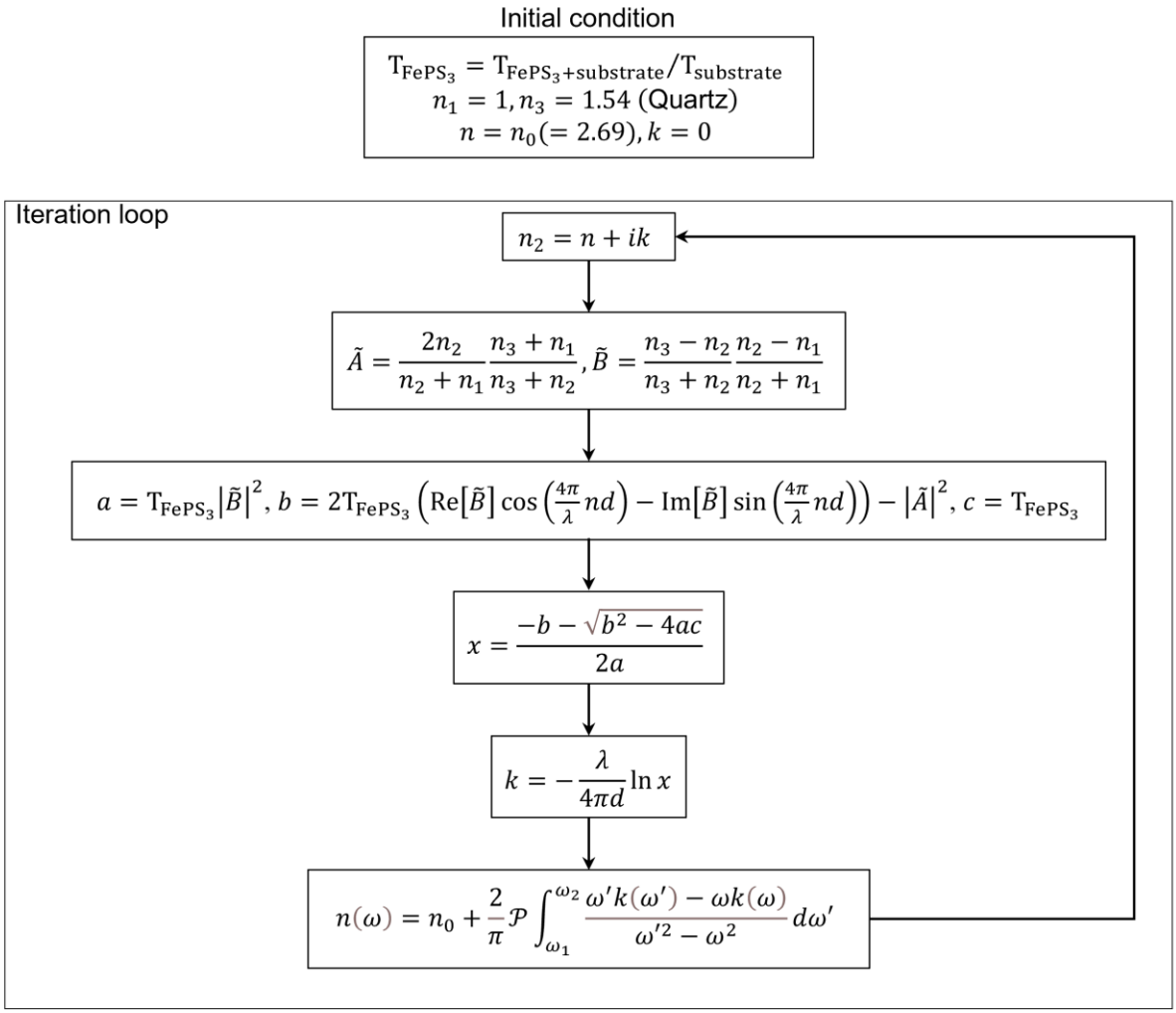

Fig. R2-6 (Reviewer only) | Procedure of n and k acquisition using low-k approximation. The optical constants (n and k) of $FePS_3$ are determined through an iterative process using its normalized transmission spectrum. Initially, $n_0 \approx 2.69$ and $k \approx 0$ are assumed, with small k retained in exponential terms to account for attenuation. The process involves solving a quadratic equation for k, updating n using the Kramers-Kronig relation, and iterating until convergence. See **Methods** in the revised manuscript for a detailed description.

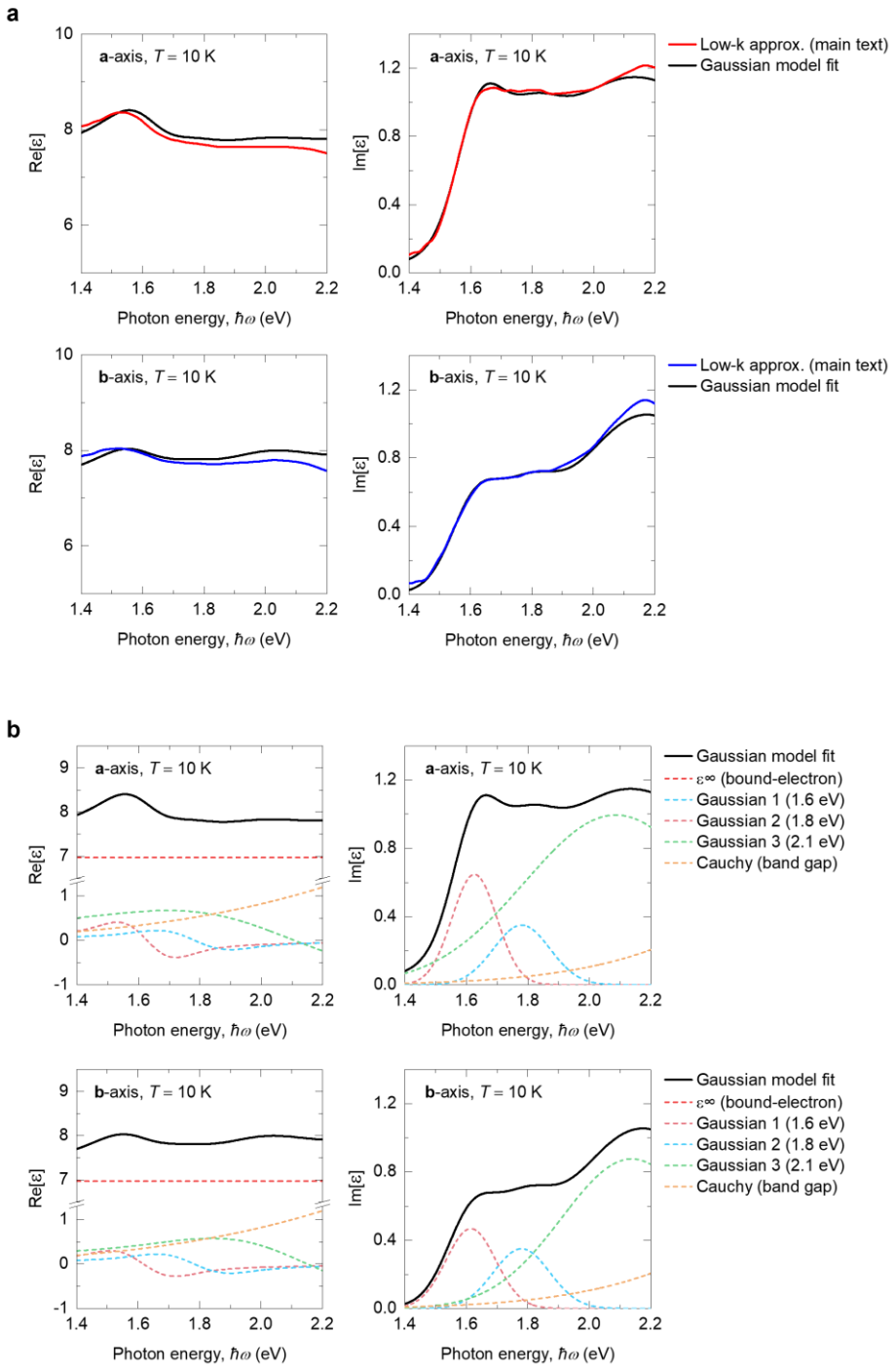

Fig. R2-7 (new Supplementary Fig. S6 in the revised manuscript) | Calculation of complex dielectric constant of a, b axes at 10 K. a, Comparison of dielectric constants obtained through two different approaches: i) Low k approximation used for the results in the mains text and ii) Gaussian fitting for comparison. Real part (left) and imaginary part (right) of the dielectric constant for the **a** direction (top) and the **b** direction (bottom). **b**, Details of optical constants model fitting, which is composed of three Gaussian models and one Cauchy model.

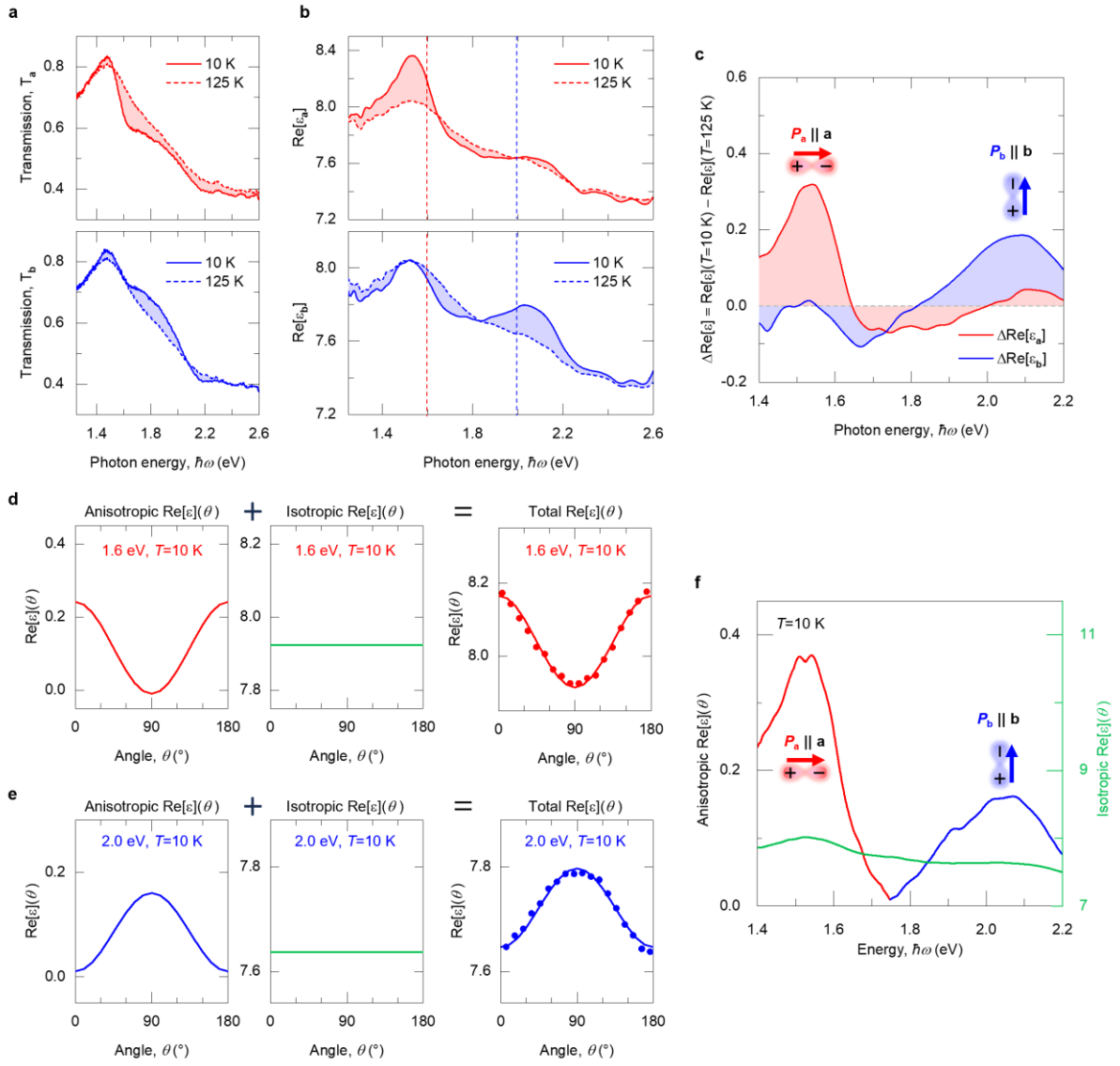

Fig. R2-8 (new supplementary Fig. S1 in the revised manuscript) | Assignment of anisotropic polarizations: $P_{a(b)}$ in the a(b) direction. a, Raw transmission spectra at T = 10 K (solid lines) and T = 125 K (dashed lines) for light polarized along the **a** and **b** directions. **b**, Calculated dielectric constant at 10 K and 125 K for light polarized along the a and b directions. Re denotes the real part. **c**, Dielectric constant difference (△Re[ε] = Re[ε] (10 K) - Re[ε] (125 K)): along the **a** direction (red line) and along the **b** direction (blue line). The emergence of $\mathbf{P}_a$ and $\mathbf{P}_b$ is schematically illustrated below. **d**,**e**, Angle-resolved dielectric constant at 10 K for 1.6 eV (**d**) and 2.0 eV (**e**). The total dielectric constant (right panels) is a superposition of isotropic (middle panels) and anisotropic polarizations (left panels). The anisotropic polarization at 2.0 eV is out of phased to that at 1.6 eV. **f**, Energy dependence of anisotropic (red and blue lines) and isotropic (green line) polarizations.

We would like to demonstrate why multipole Lorentzians are not functioning correctly, even though we were able to successfully substitute the low-k approximation for the model fitting. First, we used five Lorentzians to fit the data without any restrictions (Fig. R2-9). The experimental data does not match the fitting results with large wiggles. Additionally, there is a physical nonsense discrepancy between the center frequencies for the two axes.

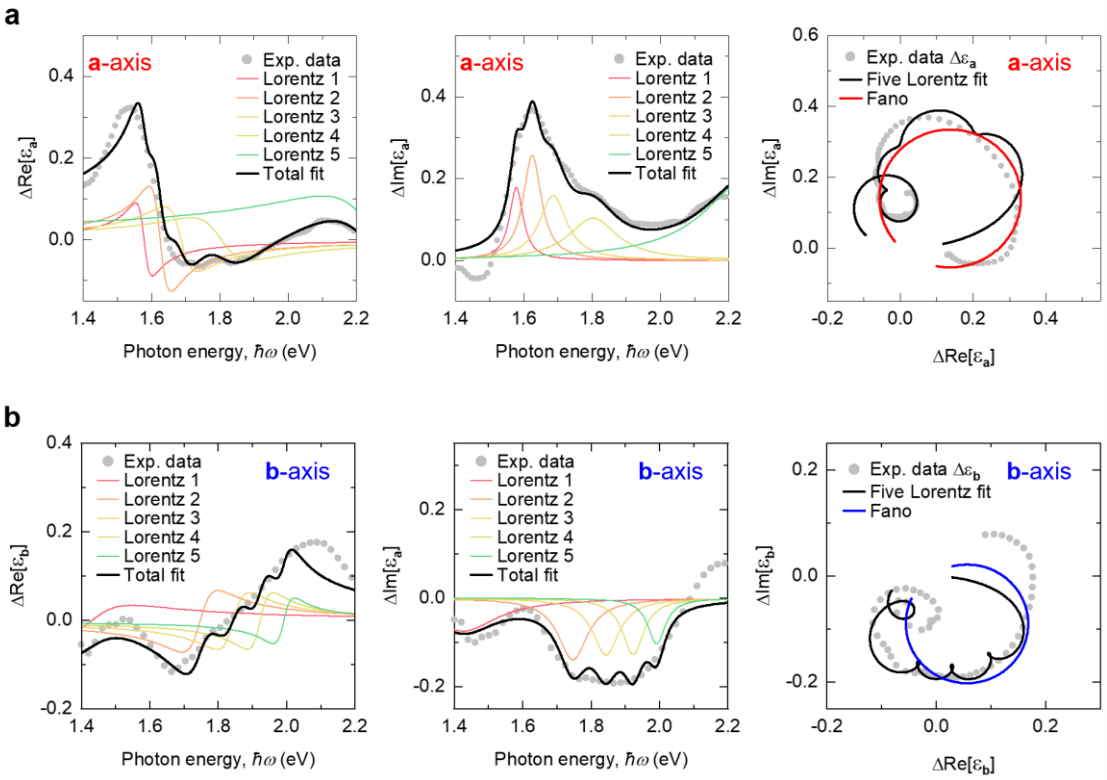

Fig. **R2-9 (Reviewer only) | Model fitting with five Lorentzian oscillators without any constraint.** a,b The fitting results in the a and b direction, respectively.

Next, using five Lorentzians with constraints on the center frequencies of both axes, we attempted to fit the data (Fig. R2-10). Only one axis of the experimental data is adequately described by the fitting results (good for an axis but bad for b axis, or vice versa). In this instance, the constraint causes four of the five Lorentzians for the b axis to become insignificantly small. Even though there is only one Lorentzian left, the fitting result differs significantly from the experimental data.

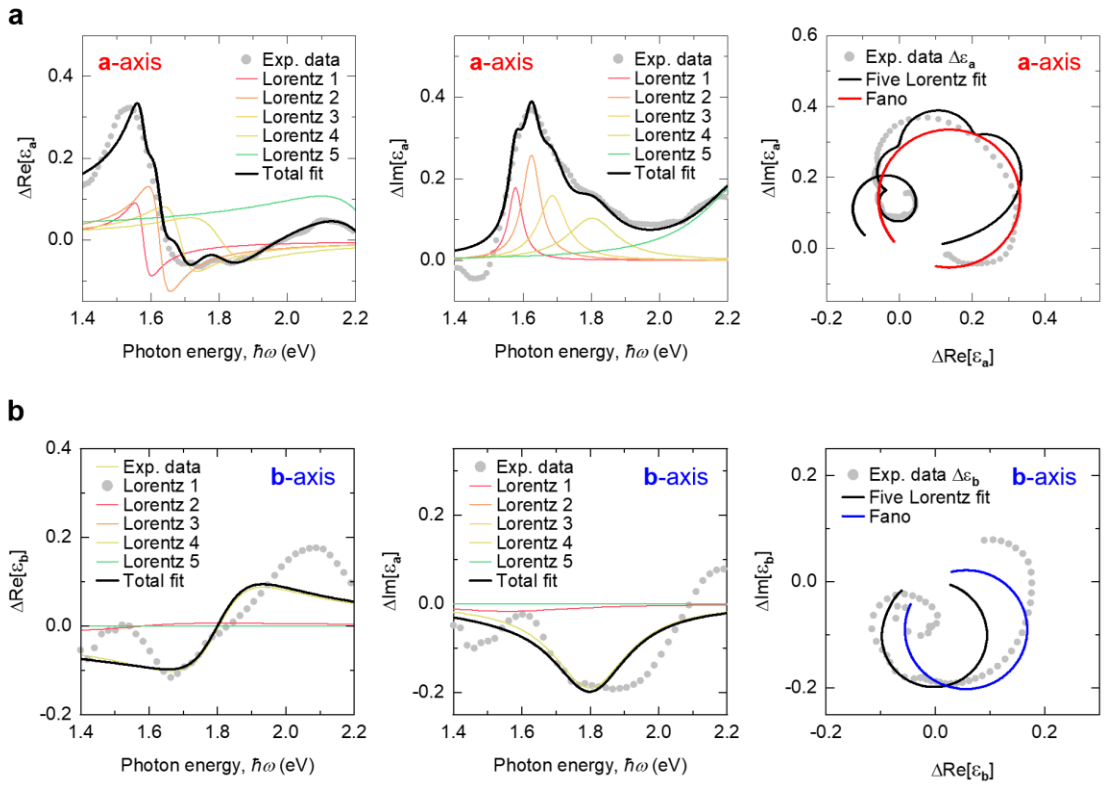

R2-10 (Reviewer only) | Model fitting with five Lorentzian oscillators without any constraint. a,b The fitting results in the a and b direction, respectively.

Thanks to your comment, we are sure that the revised manuscript is now away from the confusion.

7. The authors need to clarify the origin of the red/blue shift of the Lorentzian peak depending on the thickness in Figures 5c and d. Furthermore, the fitted Lorentzian peak does not match the experimental data, especially in Figure 5c.

Reply) We apologize for the misunderstanding. The apparent red/blue shift is not a true shift but rather a consequence of the thickness-dependent strength of quantum LB and LD. We altered the presentation in the updated manuscript to prevent any misunderstandings. The characteristic energies U-J and U+J are represented by the center frequencies of △k spectra, which we directly extract in this case (see Fig. R2-10).

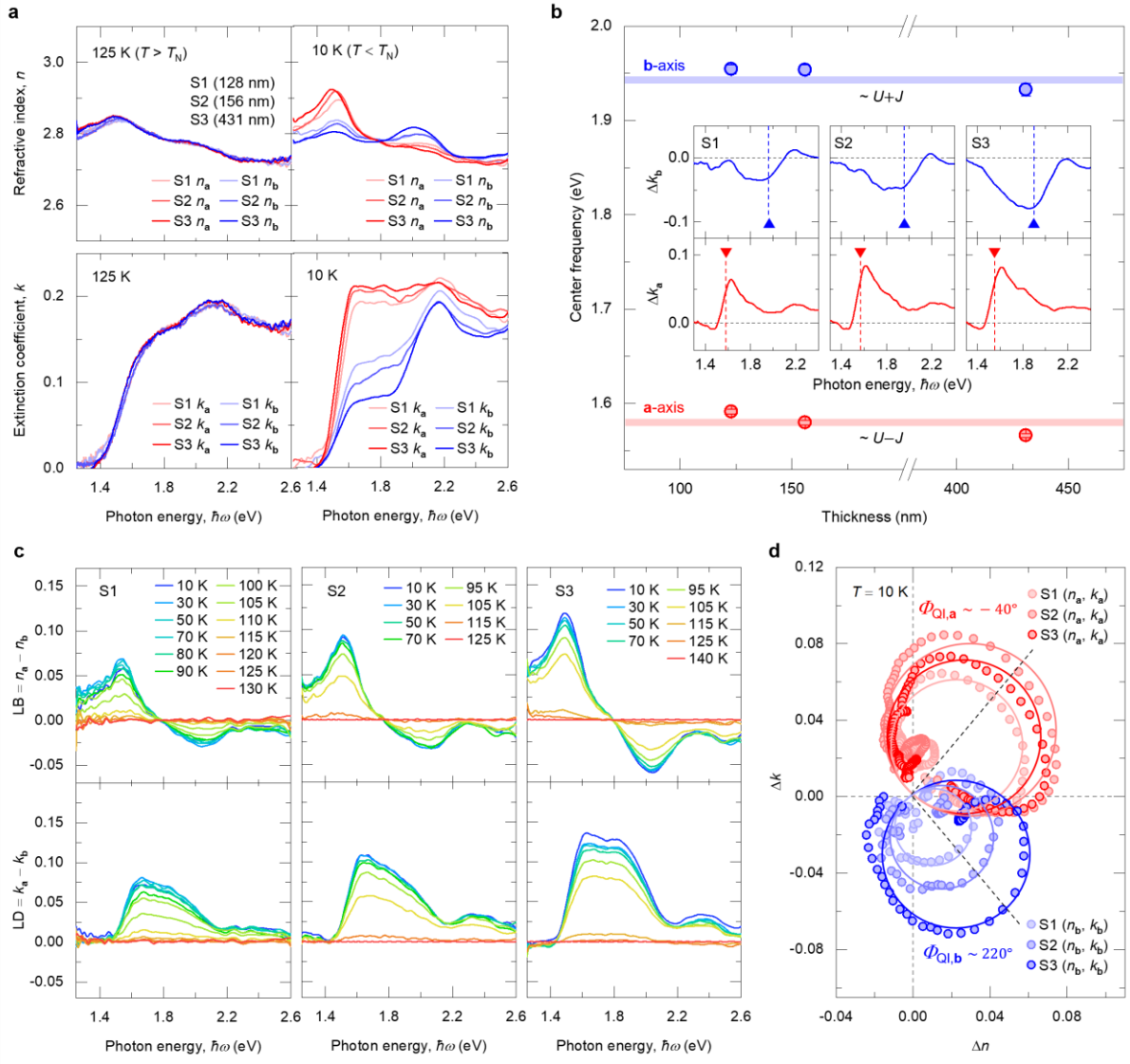

Fig. R2-10 (modified Fig. 4 in the revised manuscript) | Thickness dependence of quantum anisotropy. a, The refractive index (n) and extinction coefficient (k) for three samples with different thicknesses (S#1 with 128 nm, S#2 with 156 nm, and S#3 with 431 nm). Above T_N, both n and k are nearly identical for three samples. However, below T_N, the level of anisotropy depends on the sample thickness. **b**, The *d-d* transition peaks exhibit nearly identical splitting for all three samples. The values of U–J and U+J are estimated from the peak (dip) positions in the △k spectra

in the **a** (**b**) direction below T_N (inset).**c**, Temperature-dependent linear birefringence (LB) and linear dichroism (LD) for three samples. **d**, $\triangle n$, $\triangle k$ on the complex plane for three samples at 10 K. Dots are experimental data, and circular lines are fitting results with our quantum interference model. Red color for the **a** direction and blue color for the **b** direction. The tilting angles (namely, Φ_{QI}) of the circular contour are nearly identical for all the samples.

8. For minor points, the referencing style should be consistent throughout the manuscript.

Reply) We thank you for the suggestion. In the revised manuscript, we have corrected the reference style in a consistent manner, according to the format of Nature Communications. We are grateful for the reviewer's thoughtful comments and their dedication to improving our manuscript, even including the mechanical errors.

REVIEWER COMMENTS

Reviewer #1 (Remarks to the Author):

I appreciate the authors' detailed responses and their efforts in revising the manuscript based on my feedback. In both the response and the revised manuscript, the authors have effectively elaborated on the thickness and wavelength dependence of the refractive index, as well as the role of quantum interference effects in this material during light-matter interactions. The revised manuscript is also well-organized and more comprehensible than the previous version. I believe that all my concerns have been thoroughly addressed, and I am confident that this work will make a significant contribution to the field of light-matter interaction, both in the linear and non-linear regimes. Therefore, I recommend the manuscript for publication in Nature Communications.

Reply) We sincerely appreciate Reviewer #1's positive evaluation and recommendation for publication. We are particularly grateful for his/her insightful comments, given his/her expertise in light-matter interactions across both linear and non-linear regimes. We believe that his/her valuable feedback will significantly enhance the manuscript's impact and provide valuable insights for a broader audience interested in light-matter interactions.

Reviewer #2 (Remarks to the Author):

The authors have adequately addressed most of my comments. However, to fully address comment #2, the authors need to demonstrate the quantum interference effect experimentally in both a very thin sample (nearly monolayer) and a thick sample (approximately 1 μm). Currently, Fig 4 and S11 include only three data points (128 nm, 156 nm, and 431 nm), which is insufficient for a reliable linear fit in Fig S11. I recommend adding more data points, particularly at the extreme thicknesses, to strengthen the analysis. After this modification, I can recommend the work for publication.

Reply) We sincerely appreciate the positive feedback received from Reviewer #2. We are pleased to note that Reviewer #2 acknowledges that most of their comments have been adequately addressed.

To fully address the remaining concern, we have expanded the experimental data by including measurements on samples with varying thicknesses: d = 41 nm (thin limit), d = 290 nm, and d = 547 nm (thick limit). These additional data demonstrate 1) consistent quantum interference phase (Φ_{QI}) across different thicknesses (see Fig. R1 and revised Fig. 5), and 2) a clear linear dependence of the quantum interference effect on sample thickness (see Fig. R2 and revised Fig. S11). To avoid complications, we did not overlap it in Fig. 4 in the revised manuscript. Instead, we newly included the corresponding data (Δn and Δk on the complex plane) in the revised Fig. S11.

Due to the limited lateral size of exfoliated samples thinner than 10 nm (smaller than our beam spot size), we were unable to include data for the monolayer limit. Furthermore, we found that the experimental setup (focal point) requires adjustments for samples thinner than 30 nm, hindering direct comparison with thicker samples.

Despite these limitations, our experimental results clearly support our claim within the measured thickness range (40 nm to 0.5 μm over an order of magnitude). To reflect these findings, we have revised the manuscript to avoid extrapolating the linear fitting to the monolayer limit. Furthermore, we explicitly acknowledged the limitations of our experiments for ultrathin films (below 40 nm) in the supplementary figure caption (Fig. S11). Also, we modified the sentence prior to the discussion section from "The thickness dependence of quantum anisotropy offers an intriguing opportunity to engineer and control the strength of quantum interference effects, enabling the exploration of new phases of matter, from bulk to monolayer limits. " to "The thickness dependence of quantum anisotropy offers an intriguing opportunity to engineer and control the strength of quantum interference effects, enabling the exploration of new phases of matter, from bulk to thin limits."

Accordingly, we are confident that the current revision adequately addresses all of Reviewer #2's valuable comments. We thank you again for your valuable comments, which will significantly enhance the manuscript's impact and provide valuable insights for a broader audience interested in light-matter interactions.

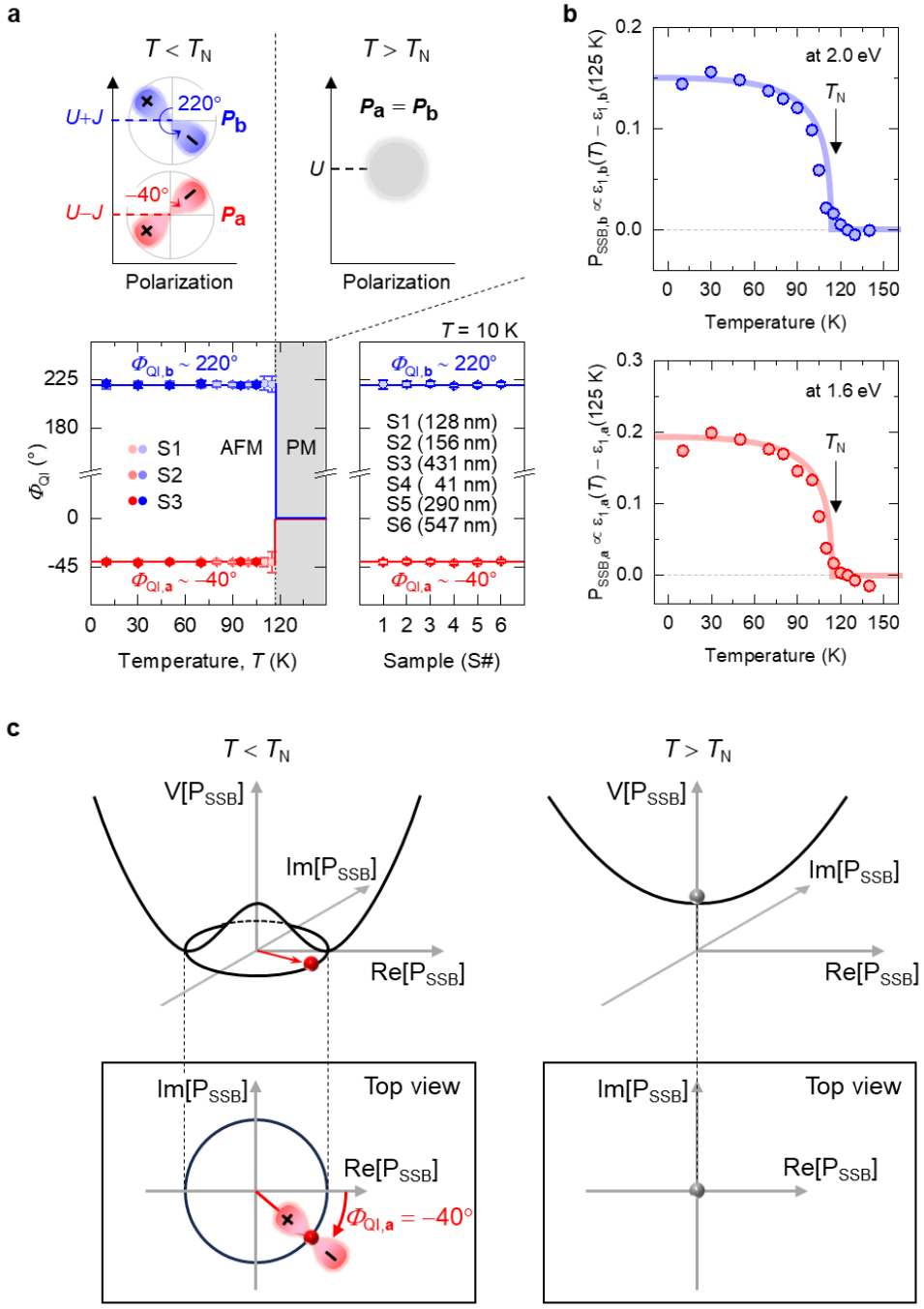

Fig. R1 (revised Fig. 5 in the manuscript) | Quantum interference-induced quantum phase transition. a, (Left panel) Temperature independence of quantum interference-induced phase (Φ_{QI}) for three samples. (Right panel) Thickness independence of Φ_{QI} measured at 10 K for six samples. (Top panels) Below T_N, the Φ_{QI} value is represented by a rotation of the light-induced electronic polarization **P** on the complex plane. At *U+J*, the polarization in the **b** direction ($\mathbf{P_b}$) is rotated by $\Phi_{QI,b}$ = 220˚. At *U–J*, the polarization in the **a** direction ($\mathbf{P_a}$) is rotated by $\Phi_{QI,a}$ = –40˚. Here, we set the direction of the **P** vector from – to +. Above T_N (paramagnetic phase), both $\mathbf{P_a}$ and $\mathbf{P_b}$ are degenerate, without pointing to a certain direction on the complex plane. Dots are experimental data and lines are guides to the eyes. The fitting error bar is extracted from the 95% confidence interval. **b**, Phase transition of

the dipole moments across T_N. The light-induced $\mathbf{P}_{SSB,a}$ and $\mathbf{P}_{SSB,b}$ are obtained from the change in the dielectric constant $\varepsilon_{1,a}$ and $\varepsilon_{2,b}$, according to the fact that **P** is proportional to ε. **c**, Quantum anisotropy due to spontaneous symmetry breaking below T_N. Below T_N, the system is described by Mexican hat potential where the energy minima are infinitely degenerate along the circular rim, distinct from the conventional parabolic potential above T_N. For $FePS_3$ below T_N, the order parameter-like $\mathbf{P}_{SSB}$ is spontaneously pointing at $\Phi_{QI,a} = -40^\circ$ for the **a** direction (bottom left panel) while no preferred angle of **P** at the center of the potential (bottom right panel) above T_N.

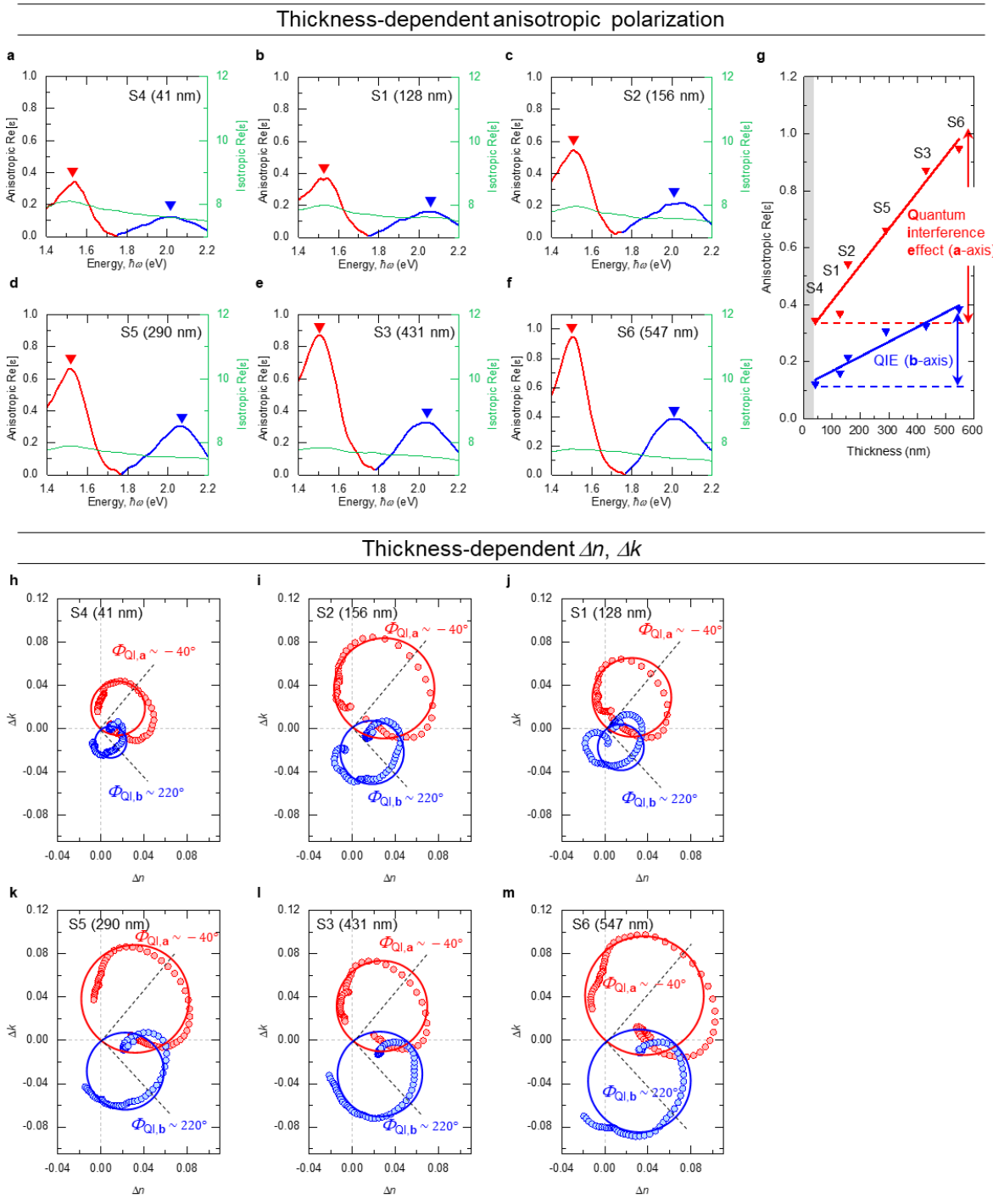

Fig. R2 (revised Fig. S11 in the supplementary materials) | Thickness-dependent anisotropic polarization. a-f, Real part of the dielectric constant (Re[ε]) for three samples (S1-S6) with different thicknesses. The red and blue lines represent the anisotropic Re[ε] along the **a** and **b** directions, respectively. The red and blue triangles indicate the peak positions. The green lines represent the isotropic Re[ε], which are nearly identical for all six samples. **g**, Thickness dependence of the anisotropic Re[ε]. The dashed line represents the estimated anisotropic Re[ε] without quantum interference effects (QIE), which is expected to be thickness independent. The solid lines show the nearly linear trend of the anisotropic Re[ε]

with quantum interference effects, with red and blue lines corresponding to the **a**-axis and **b**-axis, respectively. The linear trend is clear over the thickness range from ~40 nm to ~550 nm. Our measurements are not suitable for ultrathin films below 30 nm (shaded region). This limitation arises from two factors: 1) sample size constraints; exfoliated samples thinner than 10 nm often exhibit lateral dimensions smaller than our beam spot size, preventing reliable data acquisition for the monolayer limit and 2) experimental setup limitations; our experimental setup (focal point) necessitates adjustments for samples thinner than 30 nm, hindering direct comparison with thicker samples.